

Fragility of the free-energy landscape of a directed polymer in random media

Marta Sales¹ and Hajime Yoshino²

¹*Departament de Física Fonamental, Facultat de Física, Universitat de Barcelona, Diagonal 647, 08028 Barcelona, Spain*

²*Department of Earth and Space Science, Faculty of Science, Osaka University, Toyonaka, 560-0043 Osaka, Japan*

(Received 19 March 2002; published 28 June 2002)

We examine the sensitiveness of the free-energy landscape of a directed polymer in random media with respect to various kinds of infinitesimally weak perturbation including the intriguing case of temperature chaos. To this end, we combine the replica Bethe *Ansatz* approach outlined by Sales and Yoshino (e-print cond-mat/0112384), the mapping to a modified Sinai model, and numerically exact calculations by the transfer-matrix method. Our results imply that for all the perturbations under study there is a slow crossover from a weakly perturbed regime, where rare events take place, to a strongly perturbed regime at larger length scales beyond the so-called overlap length, where typical events take place leading to chaos, i.e., a complete reshuffling of the free-energy landscape. Within the replica space, the evidence for chaos is found in the factorization of the replicated partition function induced by infinitesimal perturbations. This is the reflex of explicit replica-symmetry breaking.

DOI: 10.1103/PhysRevE.65.066131

PACS number(s): 05.50.+q, 64.70.Pf

I. INTRODUCTION

A very interesting problem of glassy systems with disorder and frustration is the possible instability of the glassy frozen states against infinitesimally weak perturbations such as an infinitesimal change of temperatures and realizations of quenched randomness. Such a perturbation does not bring the system out of the frozen phase but possibly changes the rugged landscape of the free energy in a dramatic way. Let us call this intriguing property the *fragility of the free-energy landscape*. A class of phenomenological scaling theories started first in the context of spin glass by Bray and Moore [1] and Fisher and Huse [2,3] generically implies that equilibrium states of systems with disorder and frustration resist against such infinitesimally weak perturbations of strength $\delta \ll 1$ up to a finite crossover length scale $L_c(\delta)$ called the overlap length, but change into completely different states at larger length scales, resulting in the vanishing of the correlations between the two states. The overlap length $L_c(\delta)$ diverges as $\delta \rightarrow 0$ but remains finite for any nonzero δ . Such an anomalous response is called the *chaos*, referring to the feature that the distance between the perturbed and unperturbed systems becomes infinitely large in phase space even by infinitesimally weak perturbation as the system size L becomes macroscopically large $L/L_c(\delta) \rightarrow \infty$ [1]. Unfortunately, the validity of the prediction has not been proven explicitly by theoretical studies except for some Migdal-Kadanoff-type real-space renormalization-group studies [4,5]. Especially, the issue of *temperature chaos*, i.e., the sensitivity of glassy phases with respect to a small change of temperature, has been of great interest because of its potential relevance for the rejuvenation (chaos) effects found in temperature-shift and temperature-cycling experiments [6–8].

The majority of the previous theoretical and numerical studies concerning the problem of the fragility of glassy phases has been done on Edwards-Anderson (EA) spin-glass models, which have been considered as prototypical models for glassy systems. While a rich amount of numerical evi-

dences for the anomalous response to nonthermal perturbations has been accumulated [1,9–12], the intriguing problem of temperature chaos remains very controversial. For the Sherrington-Kirkpatrick mean-field spin-glass model, which is the EA model embedded in infinite dimensional space, it is realized that saddle point solutions both with and without temperature chaos [13–17] exist and apparently new theoretical ideas are needed. On the other hand, numerical studies report conflicting results [9,10,12,18–21].

Recently we developed an analytical scheme to study the fragility of the free-energy landscape of randomly frustrated systems against various kinds of perturbations [22]. Especially we proposed to prove the onset of chaos in terms of statistical decoupling of a set of replicated partition functions, and applied the method to the directed polymer in random media (DPRM). The DPRM [23] is a simple model compared to spin-glass models. In spite of this, it is believed to possess many of the subtle properties of glassy systems, thus, it deserves to be called “baby spin glass” [24]. Indeed, the anomalous response of DPRM towards various kinds of weak perturbations has already been reported by many numerical studies [24–28] including a signature of temperature chaos [3]. DPRM belongs to the wide class of elastic manifolds in random media [29–33], which encompasses a variety of physical systems of much interest, such as the domain walls of ferromagnets [34,35] with weak bond randomness and the flux lines in type-II superconductors with randomly distributed pointlike pinning centers [36,37], charge-density wave, and vortex lattice systems with weak random-periodic pinnings [32,38,39].

The scope of this paper is to present a unified study on the fragility of the free-energy landscape of DPRM with respect to various weak perturbations using the replica Bethe *Ansatz* approach outlined in [22], mapping to a modified Sinai model and numerically exact transfer-matrix calculations. Our main results are the following. We find that infinitesimally weak perturbations amount to replica-symmetry breaking terms in the effective action, which lead to the statistical decoupling of two sets of replicas. The outcome can be naturally understood as a manifestation of spontaneous replica-

symmetry breaking following the definition of Parisi and Virasoro [40]. Interestingly enough, the replica approach turns out to give results quite consistent with the phenomenological scaling approach [3,24–28] and predicts the same overlap length $L_c(\delta)$. Within the replica approach, apparently different perturbations can be naturally classified into a few universality classes. Concerning the well known correspondence between the effective free-energy landscape of DPRM and the Sinai model, the statistical decoupling of replicas (chaos) naturally suggests the emergence of statistically independent Sinai valleys for different subsets of replicas. To examine the anticipated universal aspects of the anomalous response, we present and discuss the outcome of a detailed numerical analysis using transfer-matrix methods.

The plan of the paper is the following. In the following sections we propose a general framework to define and study the fragility of the free-energy landscape of randomly frustrated systems. In Sec. III, we define the DPRM model. In Sec. IV, we review and summarize the previous scaling arguments. In Sec. V, we present details of the replica Bethe *Ansatz* approach outlined in [22]. Then, in Sec. VII, we present the outcome of an exhaustive numerical analysis using the transfer-matrix method. Finally, we summarize our results in Sec. VIII.

II. STATISTICAL DECOUPLING OF REAL REPLICAS

In this section we discuss a general strategy to study the sensitivity of the free-energy landscape of a generic class of systems. The free energy F of a random system is a random quantity with a certain mean and variance. Let us denote the deviation of the free energy of a given sample from the mean as

$$\Delta F = F - \overline{F}. \quad (1)$$

Here and hereafter, $\overline{(\dots)}$ denotes the average over different realizations of randomness.

Now let us consider two systems, say A and B . Initially they are prepared as two identical copies with the same randomness, temperature, and other parameters. Such systems are called *real replicas*. We are interested in how the statistical correlation between A and B changes by introducing a perturbation of strength δ . Then it is useful to define a disorder-averaged correlation function

$$C_F(L, \delta) = \frac{\overline{\Delta F_A(L) \Delta F_B(L)}}{\sqrt{\overline{\Delta F_A^2(L)}} \sqrt{\overline{\Delta F_B^2(L)}}}. \quad (2)$$

If the correlation function vanishes at large length scales

$$\lim_{\delta \rightarrow 0} \lim_{L \rightarrow \infty} C_F(L, \delta) \rightarrow 0, \quad (3)$$

it implies that the free-energy landscape of A and B decorrelates completely. If the statistical decoupling between A and B occurs even with an arbitrarily weak perturbation $\delta \ll 1$, we say that there is *chaos*.

Now let us consider an equivalent definition of chaos, which is more suited for analytical approaches based on the replica method. Let us suppose that each of the systems A and B are replicated further into n replicas and consider the disorder-averaged partition function of the total system $Z_{A+B}^n(L)$. As noticed by Kardar [41], if an analytical continuation for $n \rightarrow 0$ is possible, the disorder average of such a partition function can be identified as the generator of cumulant correlation functions of sample-to-sample fluctuations of free energies [42]. Thus, the complete knowledge of the disorder average of the replicated partition function allows one to obtain the distribution function of sample-to-sample fluctuation of the free energy [43]. In our present context, the disorder-averaged partition function $\overline{Z_{A+B}^n(L)}$ generates cumulant correlation functions of the total free-energy as the following:

$$\begin{aligned} \lim_{n \rightarrow 0} \overline{\ln Z_{A+B}^n(L)} &= n \overline{\ln Z_{A+B}(L)} + \frac{n^2}{2} \overline{[\ln Z_{A+B}(L)]_c^2} + \dots \\ &+ \frac{n^p}{p!} \overline{[\ln Z_{A+B}(L)]_c^p} + \dots \\ &= n \overline{[-\beta_A F_A(L) - \beta_B F_B(L)]} \\ &+ \frac{n^2}{2} \overline{[-\beta_A F_A(L) - \beta_B F_B(L)]_c^2} + \dots \\ &+ \frac{n^p}{p!} \overline{[-\beta_A F_A - \beta_B F_B]_c^p} + \dots, \end{aligned} \quad (4)$$

where $[\dots]_c^p$ stands for p th cumulant correlation functions of the total free energies $-\beta_A F_A - \beta_B F_B$, with $F_A(L)$ and $F_B(L)$ being free energies of subsystems A and B , respectively, and β_A and β_B being inverse temperatures of A and B , respectively.

Obviously, the decorrelation of the free-energy fluctuations between A and B is equivalent to the factorization of the replicated partition function,

$$\lim_{\delta \rightarrow 0} \lim_{L \rightarrow \infty} \lim_{n \rightarrow 0} \overline{Z_{A+B}^n(L, \delta)} = \overline{Z_A^n(L)} \overline{Z_B^n(L)}. \quad (5)$$

Note that if the latter result holds, automatically Eq. (3) holds too. An important remark is that the order in which limits are taken is crucial to obtain sensible results: the limit $n \rightarrow 0$ *must* be taken before the thermodynamic limit $L \rightarrow \infty$ and finally the limit $\delta \rightarrow 0$ must be taken. In what follows, we will use Eq. (5) as our definition of chaos in the replica approach. We have to stress, though, that this definition is general and holds for generic random systems.

The above definition of chaos implies that it can be regarded as a spontaneous symmetry breaking phenomenon. If the perturbation is absent, A and B are equivalent and one expects the exchange symmetry $A \leftrightarrow B$ to be present. One also expects to have permutation symmetry among the replicas associated with each group A or B . Such an invariance under permutations is usually called replica symmetry in short. However, in general, it turns out that the disorder-averaged replicated partition function of the $2n$ replicas Z_{A+B}^n without any perturbation has an even higher symme-

try: it is invariant under any permutation among the $2n$ replicas. Now, if Eq. (5) holds, this higher symmetry is reduced: after having introduced a perturbation, the permutation symmetry remains at most within each subset associated with A and B . Thus, in order that this phenomena happens, the perturbation should show up in the replicated partition function as a symmetry breaking term, which tries to break the full permutation symmetry. Now, definition (5) tells us that this symmetry breaking happens even with an arbitrary weak perturbation. Therefore, chaos defined as Eq. (5) is a spontaneous replica-symmetry breaking phenomenon. We note that such a definition of replica-symmetry breaking was introduced under the name *explicit replica symmetry* first by Parisi and Virasoro [40], who tried to give a sound thermodynamic definition for the replica-symmetry breaking phenomena known in the saddle point solutions of mean-field models [44–45] of a class of glassy systems.

III. MODEL

We study DPRM in $1+1$ dimensions, which is described by the following Hamiltonian in the continuous limit,

$$H_0[V, h, \phi] = \int_0^L dz \left[\frac{\kappa}{2} \left(\frac{d\phi(z)}{dz} \right)^2 + V_0(\phi(z), z) \right]. \quad (6)$$

The scalar field ϕ represents the displacement of the elastic object at point z in a one-dimensional internal space of size L . We assume that the field ϕ is a single-valued function of z , which means that *oriented* objects with no overhangs are considered. In the following, we assume that one end of the string is fixed as $\phi(0)=0$, while the other end $\phi(L)$ is allowed to move freely. The first term in the Hamiltonian is the elastic energy, κ being the elastic constant. The random pinning media is modeled by the quenched random potential $V_0(\phi, z)$ with zero mean and short-ranged spatial correlation

$$\overline{V_0(\phi, z)} = 0, \quad \overline{V_0(\phi, z)V_0(\phi', z')} = 2D\delta(\phi - \phi')\delta(z - z'). \quad (7)$$

Many exact properties of this $(1+1)$ -dimensional model are known [23]. It is in the frozen phase at all finite temperatures in the sense that its scaling properties are always governed by the $T=0$ glassy fixed point.

We implement the basic strategy explained in the preceding section as the following. First, we start with a system of two real replicas, say A and B , whose configurations $\phi_A(z)$ and $\phi_B(z)$ are subjected to exactly the same random potential and temperature. Second, we apply small perturbations to them. In the present paper we consider five different kinds of perturbations.

(i) *Tilt field* [24]. A and B replicas are subjected to a tilting field of opposite sign $-h\phi_A(L) + h\phi_B(L)$ with $h \ll 1$.

(ii) *Explicit short-ranged repulsive coupling* [24,46]. A and B replicas are subjected to explicit repulsive short-ranged interaction $\epsilon \int_0^L dz \delta(\phi_A(z) - \phi_B(z))$ with $0 < \epsilon \ll 1$.

(iii) *Decorrelation of random potential* [25,26]. The random potential of B obtained from that of A as $V_B = (V_A$

$+ \delta V')/\sqrt{1 + \delta^2}$, where $|\delta| \ll 1$ and V' follows the same Gaussian distribution as V . Then $V_G(\phi, z) = 0$ and $V_G(\phi, z)V_G(\phi', z') = 2D_{GG}\delta(\phi - \phi')\delta(z - z')$ with $D_{AA} = D_{BB} = D$ and $D_{AB} = D/\sqrt{1 + \delta^2} < D$.

(iv) *Random tilt field*. A and B are subjected to statistically independent weak random tilt field.

(v) *Temperature difference* [3]. Slightly different temperatures $T_A = T + \delta T$ and $T_B = T - \delta T$ for A and B , respectively, with $\delta T/T \ll 1$

IV. DROPLET SCALING APPROACH

We first review and discuss the scaling approach picture [3,24–28] for the problem of the anomalous response. Let us consider a simple-minded picture consisting in the deepest valley corresponding to the ground-state configuration and many branched valleys of low- (free-) energy excitations, which, for given longitudinal size L , differ from the ground state over a transverse size $u_0(L/L_0)^\zeta$, ζ being the so-called roughness exponent. Note that we have introduced a characteristic longitudinal length L_0 , which should be understood as the Larkin length [47] beyond which pinning becomes important as well as its associated transverse length scale u_0 . The free-energy gap of these excited states with respect to the “ground state” is expected to scale typically as

$$\Delta F_L^{\text{typ}} = U_0(L/L_0)^\theta. \quad (8)$$

Here U_0 is the energy scale associated with the Larkin length and θ is the stiffness exponent which is related to the roughness exponent ζ by the exact scaling relation

$$\theta = 2\zeta - 1. \quad (9)$$

In a $(1+1)$ -dimensional system these exponents are believed to be exactly $\theta = 1/3$ and $\zeta = 2/3$ [23,34,41]. The probability distribution function of the free-energy gap ΔF_L is expected to have a natural scaling form

$$\rho_L(\Delta F_L)d(\Delta F_L) = \tilde{\rho} \left(\frac{\Delta F_L}{U_0(L/L_0)^\theta} \right) \frac{d(\Delta F_L)}{U_0(L/L_0)^\theta} \quad (10)$$

with a nonvanishing amplitude at the origin,

$$\tilde{\rho}(0) > 0, \quad (11)$$

which allows rare, gapless excited states [3,24].

Let us now consider a generic perturbation which triggers an excitation from the ground state with a *free-energy gain* of order

$$\delta U \left(\frac{L}{L_0} \right)^\alpha \quad (12)$$

in the *infinitesimally weak perturbation limit*

$$\delta U/U_0 \rightarrow 0. \quad (13)$$

In the following we consider perturbations such that $\alpha > \theta$. Under the influence of such a perturbation, the system in the

deepest valley may jump into other valleys with a free-energy gap ΔF if the possible gain of free energy due to perturbation (12) becomes larger than the original free-energy gap itself. The probability of such an event is estimated as

$$p_{\text{jump}}(L, \delta U) = \int_0^{\delta U(L/L_0)^\alpha} \rho_L(\Delta F_L) d\Delta F \sim \left(\frac{L}{L_c(\delta U)} \right)^{\alpha-\theta} \quad (14)$$

with a characteristic length scale called *overlap length*,

$$L_c(\delta U) \sim L_0 \left(\frac{\delta U}{U_0} \right)^{-1/(\alpha-\theta)} \quad \text{as } \delta U/U_0 \rightarrow 0. \quad (15)$$

Let us also define a characteristic transverse length scale which is conjugate to $L_c(\delta U)$,

$$u_c(\delta U) = u_0 \left(\frac{L_c(\delta U)}{L_0} \right)^\zeta. \quad (16)$$

It is important to note that the above expressions make sense only for short enough length scales $L \ll L_c(\delta U)$. In this regime the effect of the jumps on physical quantities can be analyzed in a perturbative way because the probability of a jump is small enough. Let us call this regime the *weakly perturbed regime*. However, in the *strongly perturbed regime* $L \gg L_c(\delta U)$, perturbative treatments will fail because jump events will happen with probability one. The latter implies that after having applied the perturbation the free-energy landscape is drastically different from the original on length-scales larger than the overlap length. The overlap length (15) diverges as $\delta U/U_0 \rightarrow 0$ with exponent $-1/(\alpha-\theta)$, which is sometimes called a chaos exponent [48], but remains finite for arbitrary small strength of perturbation δ .

A. Uniform tilt field

We first consider the application of a uniform tilt field h to the end point of the real replica B at $z=L$ by which the statistical rotational symmetry is violated. In the presence of the tilt field the Hamiltonian becomes

$$H_{A+B} = H_0[V_0, \phi_A] + H_0[V_0, \phi_B] - h_{\text{uni}} \int_0^L dz \frac{d\phi_B(z)}{dz}. \quad (17)$$

The unperturbed Hamiltonian H_0 is given in Eq. (6). If the string makes a jump responding to the uniform tilt field over a distance of order $u_0(L/L_0)^\zeta$ into the next valley, it obtains an energy gain of order $h_{\text{uni}}u_0(L/L_0)^\zeta$. Thus, the unit for the gain in energy (12) reads as $\delta U = h_{\text{uni}}u_0$ with a characteristic exponent $\alpha = \zeta = 2/3$. Therefore, we find the overlap length (15) to be

$$L_c(h_{\text{uni}}) \sim L_0 \left(\frac{h_{\text{uni}}u_0}{U_0} \right)^{-3}. \quad (18)$$

This result was previously obtained by Mézard in [24] by using essentially the same argument and supporting his result by a numerical transfer-matrix calculation.

B. Explicit repulsive coupling

The other perturbations that we consider do not break the statistical rotational symmetry. First we consider the case of having a short-ranged repulsive coupling between the two real replicas by which the total Hamiltonian becomes

$$H_{A+B} = H_0[V_0, \phi_A] + H_0[V_0, \phi_B] + \epsilon \int_0^L dz \delta(\phi_A(z) - \phi_B(z)) \quad (19)$$

with $\epsilon > 0$.

This type of perturbation was first considered by Parisi and Virasoro [40] in the context of spin-glass models in order to give a precise definition of spontaneous replica-symmetry (RS) breaking. It explicitly breaks the RS noted in Sec. I. It was also used in the DPRM problem by Parisi in [46] and was further examined by Mézard using the numerical transfer-matrix method [24].

If the two replicas jump into different valleys to avoid touching each other, the energy is reduced by an amount of order $\epsilon(L/L_0)$. Thus, we read off $\alpha = 1$ and $\delta U = \epsilon$ so that the overlap length (15) becomes

$$L_c(\epsilon) \sim L_0 \left(\frac{\epsilon}{U_0} \right)^{-3/2}. \quad (20)$$

Again this length scale agrees with the result obtained by Mézard for the same quantity in [24].

C. Potential change, random tilt field, and temperature change

Now we introduce three other kinds of perturbations that do not break rotational symmetry. As we explain in Sec. V, this class of perturbations also breaks the RS noted in Sec. I. However, the strength of perturbation is subextensive $\sim L^{1/2}$ ($\alpha = 1/2$), and much weaker than in the case of explicit repulsive coupling, which is extensive $\sim L$ ($\alpha = 1$).

1. Potential change

We consider three different perturbations of $\alpha = 1/2$. The first one is to introduce a small difference between the realizations of the pinning potential for A and B [25–28]. Suppose that A has a certain realization of the pinning potential V_0 . Then we can construct the potential for B as the sum of V_0 and a new statistically independent random number V_1 . Then the total Hamiltonian becomes

$$H_{A+B} = H_0[V_0, \phi_A] + H_0[(V_0 + \delta V_1)/\sqrt{1 + \delta^2}, \phi_B]. \quad (21)$$

Here δ is the strength of the perturbation and V_1 has the same statistical properties as V_0 given in Eq. (7). Namely, it has zero mean and short-ranged correlations,

$$\overline{V_1(\phi, z)V_1(\phi', z)} = 2D\delta(\phi - \phi')\delta(z - z'),$$

$$\overline{V_0(\phi, z)V_1(\phi', z')} = 0. \quad (22)$$

Note that the pinning potential for replica B is normalized by the factor $1/\sqrt{1 + \delta^2}$, so that it has the same amplitude as replica A.

The characteristic fluctuation of the extra energy gain along a configuration due to the random variation of the potential scales typically as $\delta U_0\sqrt{L/L_0}$ since it gives contributions with random signs. Thus, we read off $\alpha = 1/2$, $\delta U = \delta U_0$ and the the overlap length (15) becomes

$$L_c(\delta) \sim L_0\delta^{-6}. \quad (23)$$

This length scale was found by Feigel'man and Vinokur by essentially the same argument [26]. Previous numerical calculations [25,28] appear consistent with it but the anticipated crossover phenomena had remained to be clarified.

2. Random tilt field

Similarly, we consider the application of a random tilt field to the end point of B ,

$$H_{A+B} = H_0[V_0, 0, \phi_A] + H_0[V_0, 0, \phi_B] - \delta \int_0^L dz h(z) \frac{d\phi_B(z)}{dz}. \quad (24)$$

Here δ is the strength of the perturbation and $h(z)$ is a Gaussian random number with zero mean and short-ranged correlations,

$$\overline{h(z)} = 0, \quad \overline{h(z)h(z')} = 2\delta(\phi - \phi')\delta(z - z'). \quad (25)$$

Within the lattice model we study numerically, the energetic gain of energy typically scales again as $\delta U_0\sqrt{L/L_0}$. Thus, we find $\alpha = 1/2$ and $\delta U = \delta U_0$, which gives the overlap length

$$L_c(\delta) \sim L_0\delta^{-6}, \quad (26)$$

3. Temperature change

All perturbations discussed so far are nonthermal perturbations. Finally we consider the introduction of a slight temperature difference between the two real replicas A and B ,

$$T_A = T + \delta T_A,$$

$$T_B = T + \delta T_B, \quad (27)$$

where $\delta T_A \neq \delta T_B$. Although this perturbation appears to be rather different from the two other cases above, it is also expected to give $\alpha = 1/2$ based on the following observation.

Fisher and Huse [3] conjectured that valley-to-valley fluctuations of the energy and the entropy are just that of a sum of random variables put on a string of length L . Thus the amplitude of valley-to-valley fluctuation scales as

$$\Delta S(L) \sim k_B(L/L_0)^{1/2},$$

$$\Delta E(L) \sim U_0(L/L_0)^{1/2}. \quad (28)$$

However, it is argued that the free energy is optimized so that these wild fluctuations cancel with each other as much as possible in such a way that valley-to-valley fluctuations of the free energy are much smaller,

$$\Delta F(L) = U_0(L/L_0)^\theta \quad \text{with} \quad \theta < 1/2. \quad (29)$$

In other words, there is a strong *negative* correlation between the fluctuations of entropy and energy such that

$$(\Delta S/k_B)(\delta E/U_0) \sim -(L/L_0) < 0 \quad (30)$$

due to the thermodynamic relation $\Delta F = \Delta E - k_B T \Delta S$. Note that a similar argument lies at the heart of the droplet theory for spin glasses, which suggests temperature chaos [1,2]. Actually, the exponent for the free-energy fluctuations is believed to be exactly $\theta = 1/3$, which is definitely smaller than $1/2$. Furthermore, the stronger fluctuation of entropy and energy (28) was confirmed numerically by a transfer-matrix calculation while the smaller fluctuation of free energy with $\theta = 1/3$ was also observed simultaneously [3,49]. Then under a slight temperature difference between the two replicas A and B , it is possible that one of the replicas jumps into a different valley taking advantage of the large gain in entropy. Such a gain should typically scale as $k_B|\delta T_A - \delta T_B|(L/L_0)^{1/2}$ and, therefore, $\alpha = 1/2$ and $\delta U = k_B|\delta T_A - \delta T_B|$. From Eq. (15), one then finds the overlap length as,

$$L_c(\delta T) \sim \left(\frac{k_B|\delta T|}{U_0} \right)^{-6} \quad (31)$$

with $\delta T = \delta T_A - \delta T_B$. This length scale was found by Fisher and Huse in [3]. Indeed their transfer-matrix calculation presented in [3] suggests the existence of crossover phenomena. However, details of the scaling properties and comparison with the case of the perturbation on the potential have remained to be explored. So we try to complete the investigation in Sec. VII.

As we summarized above, what is crucial is the role of entropy. In the so-called Larkin model [47], in which the effect of pinning is modeled by quenched random forces with short-ranged correlations, entropy plays very little role and free energy is dominated by energy so that there is no temperature chaos (see [50]).

D. Moments of transverse jump distances

In order to characterize the jump events triggered by the perturbations, it is useful to introduce appropriate correlation functions. First, let us introduce the disorder average of the q th moment of the transverse distance between the end points of the two real replicas,

$$B_q(L, \delta U) = \overline{[\Phi_A(L) - \Phi_B(L)]^q}. \quad (32)$$

It was introduced and studied numerically by Zhang in [25] and continued further in [28] for the case of perturbation on the random potential. The following is an extension of the argument by Feigel'man and Vinokur described in [26].

1. Weakly perturbed regime

In the weakly perturbed regime $L \ll L_c(\delta U)$, a jump event happens with a probability smaller than 1 as given in Eq. (14). With a single event, a transverse displacement of order $u_0(L/L_0)^\zeta$ will take place. Thus, we expect

$$B_q(L, \delta U) \sim \left[u_0 \left(\frac{L}{L_0} \right)^\zeta \right]^q p_{\text{jump}}(L, \delta U) \\ \sim u_c(\delta U)^q \left(\frac{L}{L_c(\delta U)} \right)^{(q-2)\zeta + \alpha + 1}, \quad L \ll L_c(\delta U), \quad (33)$$

where in the last step we have used the scaling relation (9).

2. Strongly perturbed regime

In the strongly perturbed regime $L \gg L_c(\delta U)$, the jump events with longitudinal size $L_c(\delta U)$ and transverse size $u_c(\delta U)$ will take place with probability 1. Let us first consider the behavior of the first moment $B_1(L, \delta U)$ in this regime.

In the strongly perturbed regime, the two replicas A and B are subjected to very different free-energy landscapes. In such a situation, we expect that the two replicas A and B will make excursions independently. Thus, we expect a simple scaling form,

$$B_1(L, \delta U) = u_c(\delta U) \left(\frac{L}{L_c(\delta U)} \right)^\zeta, \quad L \gg L_c(\delta U). \quad (34)$$

However, the situation is slightly different in the case of the uniform tilt field considered in Sec. IV A, because the uniform tilt field continues to increase the separation between A and B systematically as $L \rightarrow \infty$. After making a transverse jump of order $u_0(L/L_0)^\zeta$, another jump into a further valley in the direction of the field can take place if the strength of the field h is increased further. The latter happens when the new increment of the Zeeman energy $\delta h u_0(L/L_0)^\zeta$, due to another increment of the field δh , becomes again comparable to the typical free-energy gap [51] $\Delta F^{\text{typ}}(L)$ given in Eq. (8).

$$\delta h u_0(L/L_0)^\zeta \sim \Delta F^{\text{typ}}(L). \quad (35)$$

The number of times that such a sequence of jumps occurs by increasing the field from 0 to h will typically be $h/\delta h$. Each jump will have a typical transverse size of order $u_0(L/L_0)^\zeta$. Thus, the first moment grows as

$$B_1(L, hu_0) = u_0 \left(\frac{L}{L_0} \right)^\zeta \frac{h}{\delta h} = u_c(hu_0) \left(\frac{L}{L_c(hu_0)} \right), \\ L \gg L_c(hu_0). \quad (36)$$

In the last equation, we used the scaling relation (9). Note that the first moment ($q=1$) grows linearly with L not only in the strongly perturbed regime but also in the weakly perturbed regime as one can see using $\alpha=\zeta$ in Eq. (33). Actually the linear growth of the first moment can be proved

rigorously using the statistical rotational (tilt) symmetry of the system [24,52]. This is a rather special property of the first moment. All other moments are sensitive to the crossover from weak to strong perturbation regimes.

Let us now consider higher moments $q>1$. Since jump events are *typical* in the strongly perturbed regime, we generically expect a simple relation between different moments,

$$B_q(L, \delta U) = u_c^q(\delta U) \left(\frac{B_1(L, \delta U)}{u_c(\delta U)} \right)^q, \quad L \gg L_c(\delta U), \quad (37)$$

where note that the natural unit for the q th moment is now $u_c^q(\delta U)$. Note that in the weakly perturbed regime such a simple relation between different moments does not hold because of the rareness of the jump events. The first moment obeys a scaling law such that $B_1(L, \delta U)/u_c(\delta U)$ is a function of $L/L_c(\delta U)$ also in the strongly perturbed regime as we mentioned above. This implies that the higher moments ($q>1$) obey a scaling law such that $B_q(L, \delta U)/u_c^q(\delta U)$ becomes a function of $L/L_c(\delta U)$ ($\gg 1$) in the strongly perturbed regime.

3. Summary

To summarize, we expect a generic scaling form for the behavior of the q th moment including both weakly and strongly perturbed regimes as

$$B_q(L, \delta U) = u_c^q(\delta U) \tilde{B}_q \left(\frac{L}{L_c(\delta U)} \right). \quad (38)$$

Here the scaling function presents the asymptotic forms in the weakly perturbed regime $L \ll L_c(\delta U)$ and strongly perturbed regime $L \gg L_c(\delta U)$, which we discussed above.

E. Overlap function

Another useful quantity to probe the jump events is the overlap function defined as [24,46]

$$q(L, \delta U) = \frac{1}{L} \int_0^L dz \delta(x_0(z) - x_{\delta U}(z)). \quad (39)$$

We expect it to scale as

$$q(L, \Delta U) = \tilde{q} \left(\frac{L}{L_c(\delta U)} \right). \quad (40)$$

Note that $1-q$ is essentially the probability that the string jumps to a different valley. Thus, in the weakly perturbed regime $L \ll L_c(\delta U)$, we expect that it behaves as

$$1 - q(L, \delta U) \sim p^{\text{jump}}(L, \delta U) \sim \left(\frac{L}{L_c(\delta U)} \right)^{\alpha - \theta}. \quad (41)$$

In the strongly perturbed regime $L \gg L_c(\delta U)$, we expect that q (i.e., the probability of staying in the same valley) decays

faster down to 0 as $L/L_c(\delta) \rightarrow \infty$ because the free energy landscapes of the two replicas are increasingly different there.

F. Correlation of the free-energy fluctuation

In order to probe the difference of free-energy landscapes between the perturbed and unperturbed systems, we study the correlation function (2) of the sample-to-sample fluctuations of the free energy between the two systems, which reads as

$$C_F(L, \delta U) = \frac{\overline{\Delta F(L, 0) \Delta F(L, \delta U)}}{\sqrt{\overline{\Delta F^2(L, 0)}} \sqrt{\overline{\Delta F^2(L, \delta U)}}}. \quad (42)$$

Here $\Delta F(L, 0)$ and $\Delta F(L, \delta U)$ are deviations from the mean free energy of the unperturbed and perturbed systems. A similar correlation function was studied numerically for the case of perturbation of the temperature shift in [3]. We expect it to scale as

$$C_F(L, \Delta U) = \tilde{C}_F \left(\frac{L}{L_c(\delta U)} \right), \quad (43)$$

and decay down to 0 as $L \rightarrow \infty$.

A possible functional form of the correlation function in the weakly perturbed regime $L \ll L_c(\delta)$ can be guessed by a simple argument proposed by Bray and Moore [1] for the equivalent problem in a spin-glass model. First, we are considering perturbations such that perturbed and unperturbed systems have the same statistical properties. Thus, we must have

$$\sqrt{\overline{\Delta^2 F(L, \delta U)}} = \sqrt{\overline{\Delta^2 F(L, 0)}} \sim U_0 \left(\frac{L}{L_0} \right)^\theta. \quad (44)$$

Suppose that we introduce a perturbation that scales as $\delta U(L/L_0)^\alpha$ as given in Eq. (12). Then the fluctuations of the free energy of the perturbed system have two contributions: the original fluctuation $\Delta F(L, 0)$ plus the change due to the perturbation,

$$\Delta F(L, \delta U) = \frac{1}{\mathcal{N}} \left[\Delta F(L, 0) + \delta U \left(\frac{L}{L_0} \right)^\alpha \right]. \quad (45)$$

Here \mathcal{N} is a normalization factor which assures that the statistics of the perturbed and unperturbed systems remain the same as in Eq. (44). It is assumed that the two terms between brackets in expression (45) are uncorrelated. When performing the average over the disorder, the cross terms due to the two terms in Eq. (45) cancel out to give the following scaling function for the correlation function:

$$C_F(L, \Delta U) \sim \frac{1}{\mathcal{N}} \left[1 + \left(\frac{\delta U}{U_0} \frac{L}{L_0} \right)^{2(\alpha - \theta)} \right]^{-1/2}. \quad (46)$$

For the strongly perturbed regime $L \gg L_c(\delta)$, the correlation function may decay faster.

V. REPLICAS BETHE ANSATZ APPROACH

Now let us take the replica approach introduced in Sec. II to study chaos. We start from the partition function of $2n$ replicas: A and B and their n copies. It can be expressed by a path integral over all possible configurations of $2n$ replicas labeled by two indices $G=A, B$ and $\alpha=1, \dots, n$,

$$\overline{Z_{A+B}^n(L)} = \int \prod_{G=A, B} \prod_{\alpha=1}^n \mathcal{D}\phi_{G, \alpha} \exp(-S_{A+B}[\phi_{G, \alpha}]), \quad (47)$$

where we have introduced the dimensionless effective action,

$$S_{A+B}[\phi_{G, \alpha}] = \int_0^L dz \left[\sum_{G, \alpha} \frac{\kappa}{2k_B T} \left(\frac{d\phi_{G, \alpha}(z)}{dz} \right)^2 - \frac{D}{(k_B T)^2} \sum_{G, G', \alpha, \beta} \delta(\phi_{G, \alpha}(z) - \phi_{G', \beta}(z)) \right]. \quad (48)$$

To obtain the last equation we have used Eq. (7). Here one end of each replica is fixed as $\phi_{G, \alpha}(0) = 0$, while the other end $\phi_{G, \alpha}(L)$ is allowed to move freely as we noted above.

The effective action (48) has several important symmetries. First, it has a symmetry under global rotation in the (z, ϕ) plane. Second, it is symmetric under all possible permutations among the $2n$ replicas. Let us call the latter RS for simplicity. As we explained in Sec. II our primary interest is how the RS is broken by infinitesimally weak perturbations.

Now we focus on the study of the disorder-averaged partition function $\overline{Z_{A+B}^n(L)}$. To this respect we will use the well known mapping to an n -body imaginary time quantum mechanical problem in one-dimensional space, which was also first noted by Kardar [41,42]. The advantage of this approach is that one can make use of the Bethe *Ansatz*, which provides us with the exact ground state of the quantum problem. Moreover, from the latter one gets many hints about how to construct the relevant excited states. In what follows, the main steps in this procedure are outlined to emphasize several points which will become relevant in the analysis of the perturbation. The path integral of the partition function defined in Eq. (47) through the action in Eq. (48) can be reinterpreted as that of a quantum system in imaginary time. In the absence of temperature difference between A and B , the Schrödinger equation reads as

$$-\frac{d}{dt} \overline{Z_{A+B}^n(\{x_{G, \alpha}\}, t)} = \mathcal{H}_0 \overline{Z_{A+B}^n(\{x_{G, \alpha}\}, t)}, \quad (49)$$

with the following Schrödinger operator for $2n$ bosons:

$$\mathcal{H}_0 = - \sum_{G, \alpha} \frac{k_B T}{2\kappa} \frac{\partial^2}{\partial x_{G, \alpha}^2} - \frac{D}{(k_B T)^2} \times \sum_{((G, \alpha), (G', \beta))} \delta(x_{G, \alpha} - x_{G', \beta}). \quad (50)$$

The first term represents the kinetic energy. The second term stands for attractive short-ranged interactions between the bosons where the sum is taken over all possible pairs of bosons (excluding unphysical self-interactions which are absent in lattice models).

Let us note that here we have two kinds of bosons. The bosons of A can be distinguished from those of B and vice versa while the bosons cannot be distinguished from each other within the subgroups. However, the Schrödinger operator has an even higher bosonic symmetry: it is symmetric under permutations of all the $2n$ replicas. This is nothing but the RS we mentioned above.

By integrating out the coordinates of the free ends of the string $(\{x_\alpha, G\}, L)$ while keeping the other ends fixed at $(0,0)$, we formally obtain the disorder-averaged partition function of the replicated system as

$$\begin{aligned} \overline{Z_{A+B}^n(L)} &= \int \prod_{G=A,B} \prod_{\alpha=1}^n dx_{G,\alpha} \overline{Z_{A+B}^n(\{x_{G,\alpha}\}, L)} \\ &= \sum_{\mu} e^{-LE_{\mu}} \int \prod_{G=A,B} \prod_{\alpha=1}^n dx_{G,\alpha} \\ &\quad \times \langle \{x_{G,\alpha}\} | \psi_{\mu} \rangle \langle \psi_{\mu} | \{0\} \rangle, \end{aligned} \quad (51)$$

where $|\psi_{\mu}\rangle$ and E_{μ} are the eigenstates and eigenvalues of the Schrödinger operator \mathcal{H}_0 defined in Eq. (50). In the large L (large time) limit, the partition function will be dominated by the eigenstates of the Schrödinger operator with lowest eigenvalues (energies) including the ground state.

The ground-state wave function is well known to satisfy the Bethe *Ansatz* reading

$$\begin{aligned} \langle \Psi_{\text{RS}} | \{x_{G,\alpha}\} \rangle \\ \sim \exp \left(-\lambda \sum_{((G,\alpha),(G',\beta))} \left| x_{\alpha,G} - x_{\beta,G'} \right| \right) \\ \text{with } \lambda = \kappa D / (k_B T)^3, \end{aligned} \quad (52)$$

where the sum is taken over all possible pairs among the $2n$ replicas labeled as $(G [= A, B], \alpha [= 1, \dots, n])$. The index RS stands for the fact that this wave function has RS, i.e., permutation symmetry among all $2n$ -replicas. In the following we label this state as RS.

In general, the ground state of one-dimensional n -body problems with contact interaction is constructed in the following way: the $2n$ particles are ordered and occupy a certain segment within which they are free. The global wave function consists of the product of $2n$ plane waves whose moments λ_m have to fulfill certain matching and boundary conditions which in our case result in $\lambda_m = (2n+1-2m)\lambda$ with $m = 1, \dots, 2n$. The ground-state energy is then the sum of the kinetic energy of the $2n$ free-particles,

$$E_g = -\frac{k_B T}{2\kappa} \sum_{m=1}^{2n} \lambda_m^2 = -\frac{k_B T}{2\kappa} \frac{1}{3} \lambda^2 2n(4n^2 - 1). \quad (53)$$

Although the ground state makes the most important contribution to the partition function, it may not be the only one. If one *only* takes into account the contribution of the ground state neglecting all other excited states, one would wrongly conclude from Eq. (53) and the relation (4) that only the first and third cumulants of the correlation functions of free-energy fluctuations exist. This conclusion is definitely unphysical because the second cumulant cannot be zero. Such a pathology implies existence of continuum of gapless excited states which give important contributions to the partition function.

Bouchaud and Orland [53] pointed out that the translational symmetry of the Schrödinger operator allows to construct a continuous spectrum of excited states by considering center of mass (c.m.) motion. Such an excited state with wave vector k has the form

$$\langle \Psi_{\text{RS},k} | \{x_{G,\alpha}\} \rangle = \exp \left(ik \sum_{G,\alpha} x_{G,\alpha} \right) \langle \Psi_{\text{RS}} | \{x_{G,\alpha}\} \rangle \quad (54)$$

with eigenvalue

$$E_{\text{CM}}(k) = E_g + 2n \frac{k_B T}{2\kappa} k^2. \quad (55)$$

The resultant partition function obtained by integrating out the continuous spectrum can be put into the following scaling form [42]:

$$\overline{\ln Z_{A+B}^n} = -2n\beta \bar{f}L + g(2nL^{1/3}), \quad (56)$$

where \bar{f} in the first term represents the average free-energy density. The function $g(x)$ in the second term is analytic for small x , implying that the q th cumulant of the correlation function of free-energy fluctuations scales as $L^{q/3}$. Thus, the characteristic exponent for the free-energy fluctuation, which is called the stiffness exponent (8), is obtained as $\theta = 1/3$, being consistent with extensive numerical results of transfer-matrix calculations [23] and other analytical approaches such as mapping to the noisy Burgers equation [54].

Parisi [46] pointed out another important spectrum of excited states in which replicas are grouped into *clusters* of bound states. Each cluster is supposed to be described by a Bethe-*Ansatz*-type wave function so that there is replica (permutation) symmetry within each cluster. An important assumption is that these clusters are located far enough from each other so that their mutual overlap is negligible. The latter is allowed if the transverse size of the system is infinitely large.

In our present context, we have two kinds of bosons corresponding to the two real replicas A and B , which can be distinguished from each other. Thus, it is natural to consider an excited state which consists of separate Bethe-type clusters $\langle \Psi_{\text{RS}}^A |$ for A and $\langle \Psi_{\text{RS}}^B |$ for B , with no mutual overlaps,

$$\langle \Psi_{\text{RSB}} | = \langle \Psi_{\text{RS}}^A | \langle \Psi_{\text{RS}}^B |, \quad \langle \Psi_{\text{RS}}^B | \Psi_{\text{RS}}^A \rangle = 0. \quad (57)$$

Its associated energy is readily obtained as

$$E_{\text{RSB}} = -\frac{k_B T}{2\kappa} \frac{1}{3} \lambda^2 n(n^2 - 1) \times 2. \quad (58)$$

This wave function has the reduced replica symmetry mentioned in Sec. III, i.e., it is symmetric under permutations among A and B groups and the exchange operation $A \leftrightarrow B$. We will call this state as the replica-symmetry broken (RSB) state in the following.

A very important feature is that the gap of the RSB excited state with respect to the RS ground-state energy, which is of order $O(n^3)$, becomes vanishingly small in the $n \rightarrow 0$ limit. Thus, such an excited state should be also taken into account since we must take $n \rightarrow 0$ before $L \rightarrow \infty$ in the evaluation of the replicated partition function. Presumably each cluster of bound states can have its own center of mass motion. Therefore, the RSB excited state should have the continuum of the excited states of c.m. motion similar to that associated with the RS ground state mentioned above. Then the resultant partition function $\overline{Z_{A+B}^n}$, which will be obtained by integrating out these RSB excited states and the associated continuum due to c.m. motions, may be put again into the scaling form (56). The latter will again yield $\theta = 1/3$.

To summarize, the replica symmetry is not broken but only in a *marginal* way. As suggested by Parisi [46], the role of these RSB excited states will become important if perturbations are considered. In the following we generalize the approach of [46] and exploit its implications to study the stability of the frozen phase against the various perturbations we considered in Sec. IV.

Perturbative approach by replica scaling Ansatz

Now we address the situation in which the two real replicas A and B are under infinitesimally weak perturbations. The partition function of the system under such a perturbation can be formally written as

$$\overline{Z_{A+B}^n(L)} = \int \prod_{G=A,B} \prod_{\alpha=1}^n \mathcal{D}\phi_{G,\alpha} \exp(-S_{A+B}[\phi_{G,\alpha}] - \delta S_{A+B}[\phi_{G,\alpha}]), \quad (59)$$

where the action $S_{A+B}[\phi_{G,\alpha}]$ is the original one Eq. (48), which is fully replica symmetric and the second one, $\delta S_{A+B}[\phi_{G,\alpha}]$, is the perturbation term. Suppose that we can map the problem onto the quantum mechanical one such that the corresponding Schrödinger operator becomes

$$\mathcal{H}_{A+B} = \mathcal{H}_0 + \delta\mathcal{H}, \quad (60)$$

where \mathcal{H}_0 is the original fully replica-symmetric $2n$ -boson operator given in Eq. (50) and $\delta\mathcal{H}$ corresponds to the δS in the path integral. As we will see in the following, these perturbations try to break the RS present in the original system down to the reduced symmetry: replica symmetric only within A and B subgroups. At this stage, the whole quantum problem cannot be solved exactly. However, we can obtain a useful insight into our problem by the perturbation analysis proposed by Parisi [46].

Here let us note a problem in the case of perturbation by the random tilt field considered in Sec. IV C 2. If one tries to obtain a continuous model starting from a lattice model as considered by Kardar [41], one can find that inter-replica coupling terms due to the random tilt field emerge at second order in the transverse hopping rate of the lattice string (denoted as γ in [41]). This implies that the mapping in the continuous limit to a Schrödinger equation is invalid in this case because the Schrödinger equation contains only first-order time derivatives. Thus, we do not consider this case in this section.

From standard perturbation theory we can evaluate the first-order corrections to the original ground-state energy as

$$E_{\Delta}^{\text{RS}} = -\frac{1}{3} \frac{k_B T}{2\kappa} \lambda^2 2n(4n^2 - 1) + \frac{\langle \Psi_{\text{RS}} | \delta\mathcal{H} | \Psi_{\text{RS}} \rangle}{\langle \Psi_{\text{RS}} | \Psi_{\text{RS}} \rangle}, \quad (61)$$

where the label Δ stands for the perturbation strength and $\langle \Psi_{\text{RS}} |$ is the ground-state wave function given in Eq. (52). The first term corresponds to the ground-state energy given in Eq. (53).

Following Parisi, we will consider the RSB excited state (57),

$$\langle \Psi_{\text{RSB}} | \{x_{G,\alpha}\} \rangle \propto \exp\left(-\lambda \sum_{\alpha < \beta} \left| x_{A,\alpha} - x_{A,\beta} \right| \right) \times \exp\left(-\lambda \sum_{\alpha < \beta} \left| x_{B,\alpha} - x_{B,\beta} \right| \right) \quad (62)$$

with $\lambda = \kappa D / (k_B T)^3$. This wave function has the reduced replica symmetry. At first order in perturbation theory, we can compute the energy of the RSB excited states as follows:

$$E_{\Delta}^{\text{RSB}} = -\frac{1}{3} \frac{k_B T}{2\kappa} \lambda^2 2n(n^2 - 1) + \frac{\langle \Psi_{\text{RSB}} | \delta\mathcal{H} | \Psi_{\text{RSB}} \rangle}{\langle \Psi_{\text{RSB}} | \Psi_{\text{RSB}} \rangle}, \quad (63)$$

where the first term is the energy of the unperturbed system given by Eq. (58).

Let us introduce the ratio of the contributions to the partition function $\overline{Z_{A+B}^n}$ due to the RS ground state and the RSB excited state,

$$D(n, L) \equiv (E_{\Delta}^{\text{RSB}} - E_{\Delta}^{\text{RS}})L = D_0(n, L) - \delta D(n, L), \quad (64)$$

where

$$D_0(n, L) = \frac{k_B T}{\kappa} \lambda^2 n^3 L > 0 \quad (65)$$

is the original energy gap and the correction is due to the first order perturbation

$$\delta D(n, L) = L \left(\frac{\langle \Psi_{\text{RSB}} | \delta\mathcal{H} | \Psi_{\text{RSB}} \rangle}{\langle \Psi_{\text{RSB}} | \Psi_{\text{RSB}} \rangle} - \frac{\langle \Psi_{\text{RS}} | \delta\mathcal{H} | \Psi_{\text{RS}} \rangle}{\langle \Psi_{\text{RS}} | \Psi_{\text{RS}} \rangle} \right). \quad (66)$$

In the following we call $D(n, L)$ a gap. If it is large enough, the contribution of the RSB excited state to the partition

function becomes negligible. We will find that, in general, the correction term of the gap has the form

$$-\delta D(n, L) = -\Delta n^p L < 0. \quad (67)$$

Here the symbol Δ stands for the strength of the perturbation. Most importantly, the correction term $-\delta D(n, L)/L = -n^p \Delta$ will turn out to be *negative* for all the perturbations under consideration. In what follows we will refer to p as the *order of the perturbation*, which will play a central role. More precisely, the correction to the gap $-\delta D(n, L)/L$ will contain several terms of different powers of n . Here p is the exponent of the term with the *smallest* exponent, which becomes most relevant in the $n \rightarrow 0$ limit.

If the first-order correction turns out to give a null contribution, we have to proceed to higher-order perturbation calculations, which is obviously impossible without the complete knowledge of the whole spectrum of excited states. Fortunately for all the cases except for the case of the perturbation by uniform tilt field we will find nonzero first-order corrections. Higher-order correction terms will be higher order in Δ , which will be unimportant since we are interested in the scaling properties in the infinitesimally weak perturbation limit $\Delta \rightarrow 0$. Furthermore, it is unlikely that the higher-order terms are lower orders of n . Thus, they will be irrelevant in the $n \rightarrow 0$ limit. For the case of uniform tilt field, we will fortunately find exact RS and RSB bound states of the system, which will allow the evaluation of the gap $D(n, L)$ also in this situation.

Now using Eqs. (67) and (65) in Eq. (64) we find

$$D(n, L) = D_0(n, L) \left[1 - \left(\frac{n}{n^*(\Delta)} \right)^{-(3-p)} \right], \quad (68)$$

with

$$n^*(\Delta) = \left(\frac{\Delta}{\lambda^2 k_B T / \kappa} \right)^{1/(3-p)}. \quad (69)$$

From the above result we can generalize the argument used by Parisi for the explicit repulsive case ($p = 1$) to extract the following conclusions. As far as n is integer and the strength of the perturbation Δ is small, the contribution of the RSB state becomes negligible in the thermodynamic limit $L \rightarrow \infty$. However, we have to consider the other limiting case: the $n \rightarrow 0$ limit should be taken before $L \rightarrow \infty$. Now if $p < 3$, which will turn out to be the case for all the perturbations under study, an arbitrarily small perturbation Δ will induce a level crossing at $n^*(\Delta)$ below which the contribution of RSB excited state becomes larger than that of the original ground state (RS). The result (68) matches perfectly with our definition of chaos Eq. (5), since it suggests that the partition function of the total system factorizes in the $n \rightarrow 0$ limit as

$$\lim_{n/n^* \rightarrow 0} \overline{Z_{A+B}^n} = \overline{Z_A^n} \overline{Z_B^n} \quad \text{if } p < 3 \quad (70)$$

implying a complete change of the free-energy landscape.

Now let us further exploit the above result to find a more physical picture. In the absence of perturbations, the logarithm of the replicated partition function has a functional form (56), which reads as $\ln \overline{Z_{A+B}^n} = -\beta f L(2n) + g(2nL^{1/3})$. On the other hand, Eq. (68) implies that n/n^* is another natural variable of the replicated partition function [55]. Combining the two, we conjecture the following scaling *Ansatz*:

$$\ln \overline{Z_{A+B}^n} + \beta f L(2n) = \tilde{g}(2nL^{1/3}, n/n^*) = \tilde{g}(2nL^{1/3}, L/L^*), \quad (71)$$

where we introduced a characteristic length L^* defined as

$$L^* \sim (n^*)^{-3} \sim \Delta^{-3/(3-p)}. \quad (72)$$

An interesting observation is that the $n \rightarrow 0$ limit induces the thermodynamic limit $L \rightarrow \infty$ if the variable $nL^{1/3} = x$ is fixed. Then for fixed x we expect

$$\tilde{g}(x, L/L^* \rightarrow 0) \simeq g(2x), \quad L/L^* \ll 1 \quad (n/n^* \gg 1)$$

(weak perturbation regime)

$$\tilde{g}(x, L/L^* \rightarrow \infty) \simeq 2g(x), \quad L/L^* \gg 1 \quad (n/n^* \ll 1)$$

(strong perturbation regime). (73)

The first equation means that for small enough length scales, the effect of perturbation is small and the partition function is essentially the same as that of the unperturbed system of $2n$ replicas given in Eq. (56). The second equation is the consequence of having two statistically independent systems in the limit $L \rightarrow \infty$.

From the above scaling *Ansatz*, it follows that the correlation function of the free-energy fluctuations $C_F(L)$ considered in Sec. IV F should have the scaling form $\tilde{C}_F(L/L^*)$, which goes to 0 as $L/L^* \rightarrow \infty$. Similarly the overlap function $q(L, \delta U)$ considered in Sec. IV E should also have the scaling form $\tilde{q}(L/L^*)$, which goes to 0 as $L/L^* \rightarrow \infty$. Thus, the crossover length L^* should be identified with the overlap length $L_c(\delta U)$. The above *Ansatz* implies that the decorrelation of the free-energy landscape between A and B takes place as a universal phenomenon whose features are classified according to the order of the perturbation p . In the following, we consider the perturbations considered in the previous real-space scaling argument (Sec. IV specifically) one by one based on the replica approach and evaluate the correction to the gap, Eq. (67), explicitly and extract the strength of perturbation Δ and the order of perturbation p . Interestingly enough, we will find that the two approaches give the same overlap length.

Finally let us comment on how to choose detailed forms of perturbations, which we discuss in the following. We consider perturbations such that the original symmetry is preserved as much as possible: the $2n$ -replica system remains invariant at least under permutation among n replicas belonging to the same subset A and B and exchange $A \leftrightarrow B$, i.e., the reduced replica symmetry.

1. Short-ranged repulsive coupling

Let us begin with the perturbation that introduces an explicit repulsion term between strings A and B as given by the Hamiltonian in Eq. (17). The corresponding Schrödinger operator for the replicated system can be obviously put into the form of Eq. (60)—fully replica-symmetric term + perturbation—to obtain

$$\mathcal{H}_{A+B} = H_0 + \delta\mathcal{H}$$

with

$$\delta\mathcal{H} = \frac{\epsilon}{k_B T} \sum_{\alpha=1, \dots, n} \delta(x_{A,\alpha} - x_{B,\alpha}), \quad \epsilon > 0. \quad (74)$$

Clearly the repulsive perturbing term breaks the original RS [46].

Computing explicitly the expectation value of the δ -interaction term with respect to the Bethe ground state, one obtains [46],

$$\frac{\langle \Psi_{RS} | \delta(x_{A,\alpha} - x_{B,\alpha}) | \Psi_{RS} \rangle}{\langle \Psi_{RS} | \Psi_{RS} \rangle} = \frac{\lambda}{6} (2n+1), \quad (75)$$

while

$$\frac{\langle \Psi_{RSB} | \delta(x_{A,\alpha} - x_{B,\alpha}) | \Psi_{RSB} \rangle}{\langle \Psi_{RSB} | \Psi_{RSB} \rangle} = 0. \quad (76)$$

because the bound states of A and B subsets have no overlap $\langle \Psi_{RSB} | \Psi_{RSB} \rangle = 0$ [Eq. (57)].

Thus, the correction term to the gap, Eq. (67), is obtained as

$$-\frac{\delta D(n, L)}{L} = -\frac{\lambda}{6} (2n+1) \left(\frac{\epsilon}{k_B T} \right) n. \quad (77)$$

Note that the reduced replica symmetry—permutation symmetry among n replicas belonging to the same subset plus the exchange symmetry $A \leftrightarrow B$ —is still preserved. Thus, the leading order of the perturbation (smallest power of n , which becomes most relevant in the $n \rightarrow 0$ limit) is read off as $p = 1$ and the strength of perturbation as $\Delta \sim \epsilon$. Finally, using the relation (72) we obtain the crossover length $L^* \sim \epsilon^{-3/2}$. Remarkably the latter turns out to be the same as the overlap length (20) found in the real-space scaling argument.

2. Potential change

If a slight difference of the random potential is introduced as described in Eq. (21), the corresponding Schrödinger operator of the $2n$ replica system reads as

$$\begin{aligned} \mathcal{H} = & - \sum_{G,\alpha} \frac{k_B T}{2\kappa} \frac{\partial^2}{\partial x_{G,\alpha}^2} - \frac{D}{(k_B T)^2} \sum_{(\alpha,\beta)} \delta(x_{A,\alpha} - x_{A,\beta}) \\ & - \frac{D}{(k_B T)^2} \sum_{(\alpha,\beta)} \delta(x_{B,\alpha} - x_{B,\beta}) \\ & - \frac{1}{\sqrt{1+\delta^2}} \frac{D}{(k_B T)^2} \sum_{(\alpha,\beta)} \delta(x_{A,\alpha} - x_{B,\beta}) = \mathcal{H}_0 + \delta\mathcal{H} \end{aligned} \quad (78)$$

with the symmetry breaking term

$$\delta\mathcal{H} = \frac{\delta^2}{2} \sum_{(\alpha,\beta)} \delta(x_{A,\alpha}(z) - x_{B,\beta}(z)). \quad (79)$$

Here we are in the infinitesimally weak perturbation limit $\delta \rightarrow 0$, so higher-order terms can be ignored.

A remarkable feature is that the second term of the last equation, which is the perturbation term $\delta\mathcal{H}$, is again *repulsive*. Note that the sum is taken over n^2 rather than $n(n-1)/2$ pairs. The expectation value of the δ function with respect to the RS ground state and the RSB excited state has already been computed in Eqs. (75) and (76), hence we immediately find the correction to the gap as

$$-\frac{\delta D(n, L)}{L} = -\frac{\lambda}{6} (2n+1) \frac{\delta^2}{2} n^2. \quad (80)$$

Note that this perturbation contains the reduced replica symmetry. The latter was made possible by a specific choice of the perturbation by introducing the rescaling factor $1/\sqrt{1+\delta^2}$ used in Eq. (21). We can now read off the order of the perturbation as $p=2$ and the strength of the perturbation as $\Delta \sim \delta^2$. Now using Eq. (72), we obtain the overlap length $L^* \sim \delta^{-6}$. Indeed, the latter turns out to be that obtained by the real-space scaling argument given in Eq. (23).

3. Temperature change

Now two real replicas in the same quenched random potential $V(\phi(z), z)$ are subjected to a small temperature difference.

The Schrödinger operator for the $2n$ -replica system with A at temperature T_A and B at temperature T_B is the following:

$$\begin{aligned} \mathcal{H} = & - \sum_{\alpha} \frac{k_B T_A}{2\kappa} \frac{\partial^2}{\partial x_{A,\alpha}^2} - \sum_{\alpha} \frac{k_B T_B}{2\kappa} \frac{\partial^2}{\partial x_{B,\alpha}^2} \\ & - \sum_{((G,\alpha),(G',\beta))} \frac{D}{(k_B T_G)(k_B T_{G'})} \delta(x_{G,\alpha} - x_{G',\beta}). \end{aligned} \quad (81)$$

The RS is apparently lost in the operator. Let us choose the following specific parameters of perturbation:

$$\begin{aligned}
T_A &\rightarrow T + \delta T, \\
T_B &\rightarrow T - \delta T, \\
D &\rightarrow D \left[1 - 3 \left(\frac{\delta T}{T} \right)^2 \right].
\end{aligned} \tag{82}$$

Then we can put the operator in the form

$$\mathcal{H} = \mathcal{H}_0 + \delta \mathcal{H} \tag{83}$$

with the symmetry breaking terms

$$\begin{aligned}
\delta \mathcal{H} = & - \sum_{\alpha} \frac{k_B \delta T}{2\kappa} \frac{\partial^2}{\partial x_{A,\alpha}^2} + 2 \frac{\delta T}{T} \sum_{\alpha,\beta} \frac{D}{(k_B T)^2} \delta(x_{A,\alpha} - x_{A,\beta}) \\
& + \sum_{\alpha} \frac{k_B \delta T}{2\kappa} \frac{\partial^2}{\partial x_{B,\alpha}^2} - 2 \frac{\delta T}{T} \sum_{\alpha,\beta} \frac{D}{(k_B T)^2} \delta(x_{B,\alpha} - x_{B,\beta}) \\
& + 2 \left(\frac{\delta T}{T} \right)^2 \sum_{\alpha,\beta} \frac{D}{(k_B T)^2} \delta(x_{A,\alpha} - x_{B,\beta}) + O \left(\frac{\delta T}{T} \right)^3.
\end{aligned} \tag{84}$$

In this last equation, we are considering the limit of an infinitesimally weak perturbation $\delta T/T \rightarrow 0$ to neglect higher-order terms. The expectation value of the perturbing operator with respect to the RS ground state is obtained as

$$\begin{aligned}
\langle \Psi_{\text{RS}} | \delta \mathcal{H} | \Psi_{\text{RS}} \rangle &= 2 \left(\frac{\delta T}{T} \right)^2 \frac{D}{(k_B T)^2} \sum_{\alpha,\beta} \langle \Psi_{\text{RS}} | \delta(x_{A,\alpha} \\
& - x_{B,\beta}) | \Psi_{\text{RS}} \rangle \\
&= \frac{\lambda}{6} \frac{D}{(k_B T)^2} (2n+1) 2 \left(\frac{\delta T}{T} \right)^2 n^2.
\end{aligned} \tag{85}$$

Here we have used the fact that the ground-state wave function is symmetric with respect to the exchange $A \leftrightarrow B$ plus Eq. (75). Due to the latter, the terms of order $O(\delta T)$ cancel out and we are left with the $O(\delta T^2)$ term. Note also that the sum is again taken over $n \times n$ pairs of replicas rather than $n(n-1)/2$.

On the other hand, the expectation value of the perturbing term with respect to the RSB excited state is obtained immediately as $\langle \Psi_{\text{RSB}} | \delta \mathcal{H} | \Psi_{\text{RSB}} \rangle = 0$ using Eq. (76), and the fact that RSB wave function is symmetric with respect to the exchange $A \leftrightarrow B$ and Eq. (57). Using the above results we find the correction to the gap as [56]

$$-\frac{\delta D(n,L)}{L} = -\frac{\lambda}{6} \frac{D}{(k_B T)^2} (2n+1) 2 \left(\frac{\delta T}{T} \right)^2 n^2. \tag{86}$$

Note that the resultant gap is invariant under the exchange $A \leftrightarrow B$, which was made possible by the antisymmetric direction of the change of temperature Eq. (82). From the above results, we read off the order of the perturbation as $p=2$ and the strength of the perturbation as $\Delta \sim (\delta T)^2$. Quite remark-

ably the latter used in Eq. (72) again yields the crossover length $L^* \sim (\delta T)^{-6}$, which is the same as that found by the real-space scaling argument (31).

4. Uniform tilt field

Finally we consider applying a uniform tilt h to one real replica and $-h$ to the other. The effective action describing the uniform field perturbation (17) is the following:

$$\begin{aligned}
S_{A+B}[\phi_{G,\alpha}] = & \int_0^L dz \left[\sum_{G,\alpha} \frac{\kappa}{2k_B T} \left(\frac{d\phi_{G,\alpha}(z)}{dz} \right)^2 \right. \\
& - \frac{D}{(k_B T)^2} \sum_{G,G',\alpha,\beta} \delta(\phi_{G,\alpha}(z) - \phi_{G',\beta}(z)) \\
& \left. - \frac{h}{k_B T} \sum_{\alpha} \frac{d\phi_{A,\alpha}(z)}{dz} + \frac{h}{k_B T} \sum_{\alpha} \frac{d\phi_{B,\alpha}(z)}{dz} \right].
\end{aligned} \tag{87}$$

Here not only the full permutation symmetry among the $2n$ replicas, but also the global rotational symmetry is lost due to the field. Thus, the universality of this perturbation should be very different from those discussed so far. The corresponding Schrödinger operator of the quantum mechanical problem reads as

$$\begin{aligned}
\mathcal{H} = & - \sum_{G,\alpha} \frac{k_B T}{2\kappa} \frac{\partial^2}{\partial x_{G,\alpha}^2} - \frac{D}{(k_B T)^2} \sum_{G,G',\alpha,\beta} \delta(x_{\alpha} - x_{\beta}) \\
& - \frac{h}{\kappa} \sum_{\alpha} \frac{\partial}{\partial x_{A,\alpha}} + \frac{h}{\kappa} \sum_{\alpha} \frac{\partial}{\partial x_{B,\alpha}}.
\end{aligned} \tag{88}$$

Note that the first two terms are the original operator \mathcal{H}_0 given in Eq. (50).

Now let us analyze the change of the RS state (52). One can easily see that the first-order perturbation vanishes simply because the total momentum of the ground state is zero. On the other hand, one can also easily note that when a field is applied, the original wave function is no longer an eigenstate. Fortunately, the exact eigenstate can be found in this odd situation in which particles belonging to different subsets (A and B) are driven into opposite directions. The former Schrödinger operator (88) can be rewritten into the fully symmetric form of the original problem (50) by shifting the momenta,

$$\frac{\partial}{\partial x'_{A,\alpha}} = \frac{\partial}{\partial x_{A,\alpha}} - \frac{h}{k_B T}, \quad \frac{\partial}{\partial x'_{B,\alpha}} = \frac{\partial}{\partial x_{B,\alpha}} + \frac{h}{k_B T}. \tag{89}$$

Notice that this transformation preserves the commutation relations between conjugated coordinates and moments (i.e., $[\partial/\partial x'_{G,\alpha}, x_{G,\alpha}] = [\partial/\partial x_{G,\alpha}, x_{G,\alpha}]$). In terms of these new coordinates, the RS ground state again takes the form of the

Bethe *Ansatz* solution of Eq. (52). And, therefore, the final ground state can be obtained from Bethe's wave function by undoing the previous shifting of moments,

$$\Psi \sim \Psi_{\text{RS}}(\{x_{G,\alpha}\}) \exp\left(\frac{h}{k_B T} \sum_{\alpha} x_{A,\alpha}\right) \exp\left(-\frac{h}{k_B T} \sum_{\alpha} x_{B,\alpha}\right), \quad (90)$$

where $\Psi_{\text{RS}}(\{x_{G,\alpha}\})$ is the original Bethe *Ansatz* wave function for $2n$ replicas given in Eq. (52). The eigenvalue E_h corresponding to this wave function is obtained as

$$E_h = E_0 + \frac{nh^2}{\kappa k_B T}, \quad (91)$$

which does not depend on the ordering of the particles. Here E_0 is the original ground-state energy E_g given in Eq. (53). Although the original full permutation symmetry is lost in the wave function (90), it still described a sort of bound state on $2n$ particles. So we may refer to it as the RS state. In the following section, we will discuss the mapping onto the Sinai model and the physical meaning will become clearer. The second term of Eq. (91) gives the change of the eigenvalue of the RS state due to the perturbation $\Delta E_{\text{RS}} = nh^2/(\kappa k_B T)$.

Next let us consider the change of the eigenvalue corresponding to the RSB excited state, which again is formed by two separate bound states for A and B subsets. Here it is useful to note that if *all* the particles are subjected to the common field, the unperturbed single-bound-state wave function is still an eigenstate of the operator. Based on this observation, one immediately finds that the unperturbed RSB wave function is still a valid eigenstate under the field because of a twofold reason: (i) there is no overlap between A and B and (ii) rotational and replica symmetries are preserved within the same subsets. Thus, the eigenvalue of the RSB state does not change by the perturbation $\Delta E_{\text{RSB}} = 0$.

Using the above values of ΔE_{RS} and ΔE_{RSB} we obtain

$$-\frac{D(n,L)}{L} = -\frac{nh^2}{\kappa k_B T}. \quad (92)$$

We can now read off $p=1$ and $\Delta \sim h^2$, which yields the overlap length $L_c \sim h^{-3}$. Then using Eq. (72) we find the same overlap length $L^* \sim h^{-3}$, being consistent with the result (18) of the real-space scaling argument.

VI. MAPPING TO A MODIFIED SINAI MODEL

In the preceding section, we found decorrelation of the free-energy landscapes of perturbed and unperturbed systems. Here we analyze the problem further for the case of uniform tilt field based on the connection between the $(1+1)$ -dimensional DPRM and the statistical mechanics of the Sinai model [24,46,53,57]. With this mapping, an effective one-dimensional energy landscape for the free end $x(L)$ of the $(1+1)$ -dimensional DPRM is obtained as a Sinai poten-

tial, which is generated by a simple random walk in a one-dimensional space.

Here we consider this mapping onto the Sinai model in the presence of the uniform tilt field by evaluating the partition function (51). First, we evaluate the partition function assuming the RS and using the ground-state wave function given in Eq. (90). Second, we perform another evaluation assuming RSB, which only allows reduced replica symmetry, and using the clustered wave function (62). The former is supposed to be good for the weakly perturbed regime $L \ll L_c(h)$ while the latter is good for the strongly perturbed regime $L \gg L_c(h)$. In order to interpolate the two limits, we propose a phenomenological model using a bounded Sinai potential.

A. Replica symmetric case

We start by considering the fully RS *Ansatz* following Bouchaud and Orland [53]. The ground-state wave function under a uniform tilt is given by Eq. (90). In order to take into account the motion of the center of mass (c.m.) of the $2n$ replicas, we consider the spectrum of excited states whose wave functions are given by

$$\begin{aligned} \Psi_{\text{RS}}(h,k;\{x_{G,\alpha}\}) &\sim \Psi_{\text{RS}}(\{x_{G,\alpha}\}) \\ &\times \exp\left[\frac{h}{k_B T} \left(\sum_{\alpha} x_{A,\alpha} - \sum_{\alpha} x_{B,\alpha}\right)\right] \\ &\times \exp\left(ik \sum_{G,\alpha} x_{G,\alpha}\right). \end{aligned} \quad (93)$$

The first factor is the Bethe wave function given in Eq. (52), which describes the unperturbed bound state of $2n$ replicas. Now we use the Gaussian transformation introduced by Parisi in [46] to represent Bethe's wave function as follows:

$$\begin{aligned} \Psi_{\text{RS}}(\{x_{G,\alpha}\}) &\sim \exp\left(-\lambda \sum_{((G,\alpha),(G',\beta))} \left|x_{\alpha,G} - x_{\beta,G'}\right|\right) \\ &= \int \mathcal{D}V \exp\left[-\int dx \frac{1}{4\lambda} \left(\frac{dV}{dx}\right)^2\right] \\ &\times \exp\left(\sum_{G,\alpha} \mathcal{V}(x_{G,\alpha})\right). \end{aligned} \quad (94)$$

The second factor arises from the uniform tilt perturbation: h to subset A and $-h$ to subset B . The last factor is the plane wave of wave vector k , which accounts for the free c.m. motion. Here the ground state is included as the $k=0$ case. One can easily find the eigenvalues to be

$$E_{\text{RS}}(h,k) = E_0 + \frac{nh^2}{\kappa k_B T} + n \frac{k_B T}{\kappa} k^2. \quad (95)$$

The first term is the original ground-state energy E_g of the unperturbed system given in Eq. (53), the second term is due to the perturbation, and the third term is due to the c.m. motion.

Let us now suppose that replicas have both ends fixed: one at (0,0) and the other at x_A in the case of subset A and at x_B in the case of subset B . Then the partition function (51) is evaluated by integrating out the spectrum of excited states as

$$\begin{aligned} \overline{Z_{\text{RS}}(0,0|x_A, x_B)} &\sim e^{-[E_0 + nh^2/(2\kappa k_B T)]L} \\ &\times \int \mathcal{D}\mathcal{V} \exp\left[-\int dx \frac{1}{4\lambda} \left(\frac{d\mathcal{V}}{dx}\right)^2\right] \\ &\times \exp[n\mathcal{V}(x_A) + n\mathcal{V}(x_B)] \\ &\times \exp[(h/k_B T)(nx_A \\ &+ nx_B)] \int dk \sqrt{Ln \frac{k_B T}{\kappa\pi}} \\ &\times \exp\left(-Ln \frac{k_B T}{\kappa} k^2 + ik(nx_A + nx_B)\right) \\ &\sim e^{-(E_0 + nh^2/(\kappa k_B T))L} \\ &\times \overline{[\exp\{-nL^{1/3} E_{\text{RS-Sinai}}(T, h, \mathcal{V}; y_A, y_B)\}]}_{\tilde{\mathcal{V}}}, \end{aligned} \quad (96)$$

where $\overline{[\dots]}_{\tilde{\mathcal{V}}}$ means the average over the effective potential $\tilde{\mathcal{V}}$,

$$\overline{[\dots]}_{\tilde{\mathcal{V}}} = \int \mathcal{D}\tilde{\mathcal{V}} \exp\left[-\int dy (1/4\lambda) \left(\frac{d\tilde{\mathcal{V}}}{dy}\right)^2 \dots\right] \quad (97)$$

and $E_{\text{RS-Sinai}}(T, h, \mathcal{V}; y_A, y_B)$ is the effective Hamiltonian,

$$\begin{aligned} E_{\text{RS-Sinai}}(T, h, \mathcal{V}; y_A, y_B) &= \frac{\kappa}{2k_B T} \frac{(y_A + y_B)^2}{2} + \tilde{\mathcal{V}}(y_A) + \tilde{\mathcal{V}}(y_B) \\ &\quad - \frac{\tilde{h}}{k_B T} y_A + \frac{\tilde{h}}{k_B T} y_B \end{aligned} \quad (98)$$

in terms of the scaled variables

$$x = L^{2/3} y, \quad \mathcal{V} = -L^{1/3} \tilde{\mathcal{V}}, \quad h = L^{-1/3} \tilde{h}. \quad (99)$$

By increasing $nL^{1/3}$, the partition function will be dominated by the minimum of the effective Hamiltonian $E_{\text{RS-Sinai}}(T, h, \mathcal{V}; y_A, y_B)$. Then the following physical interpretation can be made: the end points of the strings A and B are subjected to the *same effective quenched random potential* which displays the long-ranged correlations in transverse space just as the Sinai model,

$$\overline{[\{\tilde{\mathcal{V}}(y) - \tilde{\mathcal{V}}(y')\}^2]}_{\tilde{\mathcal{V}}} \propto |y - y'|. \quad (100)$$

Furthermore, the c.m. of the total system is subjected to an effective Hookian spring, which tries to bind together the two real replicas. The effect of the uniform tilt field amounts to an effective transverse force \tilde{h} applied at the end points of A and B replicas, which tries to drive them into the opposite directions. From Eq. (99), it can be seen that the effective force \tilde{h} increases by increasing the system size L (with fixed h).

B. Replica-symmetry broken case

In Sec. V A 4, we found out that replica-symmetry breaking becomes important at $L \gg L_c(h)$ with $L_c(h) \sim h^{-3}$ given in Eq. (18). Here we perform the evaluation of the partition function (51) based on the RSB *Ansatz*. In this case, we consider a spectrum of excited states whose wave functions are given by

$$\begin{aligned} \Psi_{\text{RSB}}(h, k_A, k_B; \{x_{G, \alpha}\}) \\ \sim \Psi_{\text{RS}}(\{x_{A, \alpha}\}) \Psi_{\text{RS}}(\{x_{B, \alpha}\}) \exp\left(ik_A \sum_{\alpha} x_{A, \alpha}\right) \\ \times \exp\left(ik_B \sum_{\alpha} x_{B, \alpha}\right). \end{aligned} \quad (101)$$

The first two factors are due to the original wave function of the RSB state (62), which consists in two clusters of bound states. As we noted in Sec. V A 4, it remains as an eigenstate even under the uniform tilt field since it is assumed that these clusters have zero overlap. Moreover, this absence of overlap also allows independent c.m. motions of A and B subsets. The latter two factors account for such separate c.m. motions. The eigenvalues are the following:

$$\begin{aligned} E_{\text{RSB}}(h, k_A, k_B) &= E_{\text{RSB}} + n \frac{h}{\kappa} (ik_A) + n \frac{h}{\kappa} (ik_B) + n \frac{k_B T}{2\kappa} k_A^2 \\ &\quad + n \frac{k_B T}{2\kappa} k_B^2. \end{aligned} \quad (102)$$

The first term is the original ground-state energy E_{RSB} of the unperturbed RSB state given in Eq. (58). The second and third terms come from the perturbation. The last two terms are due to the separate c.m. motions. The partition function (51) is evaluated by integrating out the spectrum of excited states as

$$\begin{aligned}
\overline{Z_{\text{RSB}}(0,0|x_A,x_B)} &\sim e^{-E_0 L} \int \mathcal{D}V_A \exp\left[-\int dx \frac{1}{4\lambda} \left(\frac{dV_A}{dx}\right)^2\right] \int \mathcal{D}V_B \exp\left[-\int dx \frac{1}{4\lambda} \left(\frac{dV_B}{dx}\right)^2\right] \\
&\times \exp[nV_A(x_A) + nV_B(x_B)] \int dk_A \sqrt{Ln \frac{nk_B T}{2\kappa\pi}} \int dk_B \sqrt{Ln \frac{k_B T}{2\kappa\pi}} \\
&\times \exp\left(-Ln \frac{2k_B T}{\kappa} k_A^2 - Ln \frac{2k_B T}{\kappa} k_B^2 - Ln \frac{h}{\kappa} (ik_A) + Ln \frac{h}{\kappa} (ik_B) + ik(nx_A + nx_B)\right) \\
&\sim e^{-[E_0 + (2n)h^2/(2\kappa k_B T)]L} \\
&\times [\exp\{-nL^{1/3} E_{\text{RSB-Sinai}}(T, h, \tilde{V}_A, \tilde{V}_B; y_A, y_B)\}]_{\tilde{V}_A, \tilde{V}_B}, \tag{103}
\end{aligned}$$

where $E_{\text{RSB-Sinai}}(T, h, \tilde{V}_A, \tilde{V}_B; y_A, y_B)$ is the effective Hamiltonian, again in terms of the scaled variables,

$$\begin{aligned}
E_{\text{RS-Sinai}}(T, h, \tilde{V}_A, \tilde{V}_B; y_A, y_B) \\
&= \frac{\kappa}{2k_B T} y_A^2 + \tilde{V}_A(y_A) - \frac{\tilde{h}}{k_B T} y_A + \frac{\kappa}{2k_B T} y_B^2 \\
&+ \tilde{V}_B(y_B) + \frac{\tilde{h}}{k_B T} y_B. \tag{104}
\end{aligned}$$

It is interesting to compare the last result with the RS one given in Eq. (98). Here the two subsets A and B are now subjected to *independent Hookian springs*, which try to confine the c.m. of each subset while the *total* c.m. was confined in the RS case. Moreover, the two replicas are now subjected to *completely independent Sinai potentials* \tilde{V}_A and \tilde{V}_B . The effect of the uniform tilt field again amounts to an effective transverse force \tilde{h} applied at the end points of replicas A and B , which tries to drive them into opposite directions just as in the replica-symmetric case.

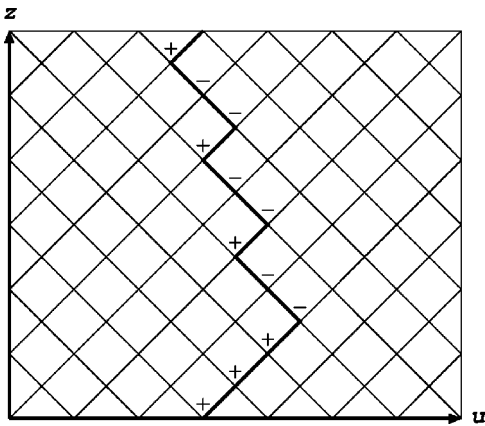


FIG. 1. The lattice (1+1)-dimensional DPRM model. This example has longitudinal size $L=12$ and transverse size $U=14$. The thick zigzag line is an example of the configuration. The string is directed in the direction of the z axis with transverse displacements in the direction of the u axis.

C. Discussion

In Sec. V, we conjectured a possible scaling form (71) of the crossover from the weakly perturbed regime at length scales shorter than the overlap length L_c , where the RS holds, to the strongly perturbed regime where replica-symmetry breaking becomes relevant,

$$\ln \overline{Z_{A+B}^n} + \beta f L(2n) = \tilde{g}(2nL^{1/3}, L/L_c). \tag{105}$$

Indeed, the partition function based on the RS and RSB *Ansätze* given in Eqs. (96) and (103) has the expected form; the $O(\overline{n})$ term which provides the average free energy $\beta f L(2n)$, plus a function which contains the two scaling variables $nL^{1/3}$ and $\tilde{h} = L^{1/3}h = [L/L_c(h)]^{1/3}$. In the last equation we used the relation $L_c(h) \sim h^{-3}$ given in Eq. (18).

Here we have only discussed the two limiting *Ansätze*: RS and RSB. The crossover between the two limits remains an open problem. Here let us propose a modified Sinai model which interpolates the limits. We define an effective Hamiltonian for the end points' positions of replicas A and B at a given length, which reads as follows:

$$\begin{aligned}
H &= H_A + H_B, \quad H_A = \frac{\kappa}{2k_B T} y_A^2 + \tilde{V}(y_A) + \tilde{h} y_A, \\
H_B &= \frac{\kappa}{2k_B T} y_B^2 + \tilde{V}(y_B) - \tilde{h} y_B, \tag{106}
\end{aligned}$$

where $\tilde{V}(x)$ is a *bounded* Sinai potential with correlations,

$$\overline{[\tilde{V}(x) - \tilde{V}(y)]^2} \propto C(|x-y|)$$

with

$$C(u) = y + (1-u)\theta(u-1). \tag{107}$$

Here the correlation grows as $C(u)=u$ for $u \leq 1$ and saturates, $C(u)=1$, for larger separations $u > 1$. The latter saturation (confined random walk) allows us to realize statistically independent Sinai valleys at large separations (RSB). Actually, such a saturation of the effective energy landscape was observed numerically in the DPRM by Mézard [24].

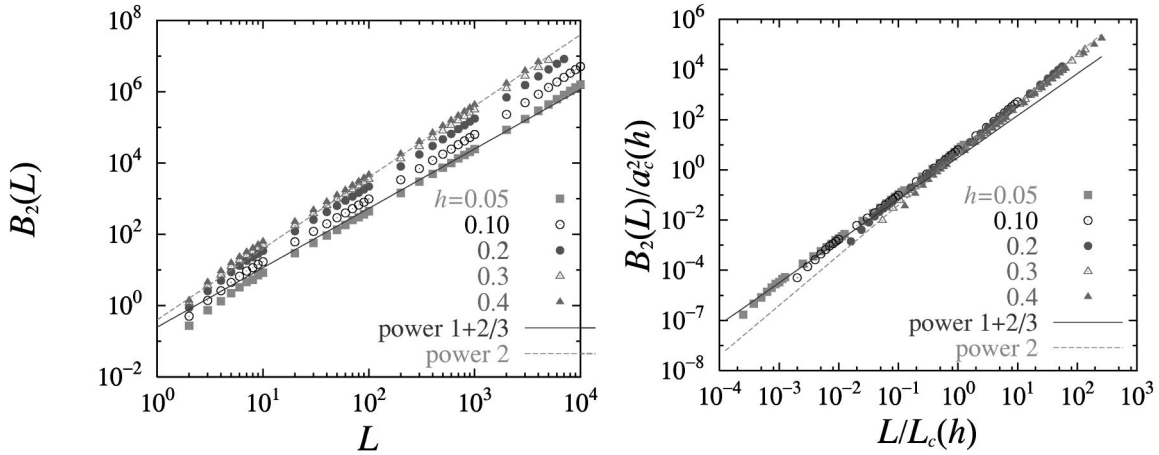


FIG. 2. $B_2(L)$ of uniform tilt field case. The data is shown on the left and its scaling plot is shown on the right. Here the scaling parameters are $L_c(h) = h^{-3}$ and $u_c(h) = L_c(h)^{\zeta=2/3}$.

In Sec. VII A we analyze the crossover phenomena in detail by a transfer-matrix method. Subsequently, in Sec. VII B, we analyze the phenomena numerically using the modified Sinai model defined above and compare the result with that obtained in the original DPRM.

VII. NUMERICAL ANALYSIS

Now we examine numerically in detail the properties of the anomalous response of the DPRM towards various perturbations discussed in the preceding sections by transfer-matrix calculations. We focus on the anticipated universal scaling properties of the crossover from the weakly to strongly perturbed regime across the overlap length, which has not been clarified in previous numerical studies (see, however, [24]).

Specifically, we consider a lattice model on a two-dimensional lattice of size $L \times U$ as shown in Fig. 1. The string of length L is directed along the z axis with transverse displacements in the direction of the u axis. The configuration of the string is represented by the positions of the vertices X which the configuration goes through, i.e., $(u(z), z)$ with $z = 1, \dots, L$. The gradient $\sigma(z) = u(z+1) - u(z)$ is constrained to take only the values $+1$ or -1 . Note that elasticity is realized entropically within this lattice model. The random potential $V(u, z)$ is defined on each vertex (u, z) on which it takes a random value drawn from a uniform distribution between $-V_0$ and V_0 . The energy of a configuration $\{u(z)\}$ is given by

$$E[V, u] = \sum_{z=1}^L V(u(z), z). \quad (108)$$

One end of the configuration is fixed at $(0, 0)$ and the other end is allowed to move freely. On the transverse direction we have imposed periodic boundary conditions such that $V(u+U, z) = V(u, z)$. The natural unit for the temperature is the scaled thermal energy $k_B T / V_0$, where V_0 is the unit for the random potential. In the following, the Boltzmann con-

stant is set to $k_B = 1$ and the unit for the random potential to $V_0 = 1$, so that we will often denote the scaled thermal energy simply as T .

First we prepare two real replicas A and B identically except for small perturbations, which we will describe in detail. Depending on the type of the problem, we use either zero temperature [34] or finite temperature versions [58] of the transfer-matrix method to compute correlation functions. Here and in the following, \bar{X} denotes the average of a quantity X over different realizations of the random potential and $\langle X \rangle$ denotes the thermal average of X (or simply the value of X at ground state in the case of zero temperature). We have examined various system sizes up to $L = 10^4$ and have averaged over $N_s = 10^4$ different realizations of the random potential except for the explicit repulsive coupling case for which we used system sizes up to $L = 10^3$ and $N_s = 10^4$. The limitation of the system size used for the latter case is that we have to take into account explicitly the inter-real-replica coupling in the transfer matrix, which requires one to keep track of trajectories of two strings simultaneously and thus much larger computational effort [24].

First, we examine the mean-squared transverse displacement of the end point due to the perturbation,

$$B_2(L) = \overline{\langle u_A(L) - u_B(L) \rangle^2}. \quad (109)$$

Here $u_A(L)$ and $u_B(L)$ stand for the position of the end points of replicas A and B , respectively. Second, we compute the exact free energies (or ground-state energies at zero temperature) of both replicas by the transfer-matrix method and examine the correlation of the free energies,

$$C_F(L) = \frac{\overline{\Delta F_A(L) \Delta F_B(L)}}{\sqrt{\overline{\Delta F_A^2(L)}} \sqrt{\overline{\Delta F_B^2(L)}}}, \quad (110)$$

where ΔF is the deviation from the mean free energy,

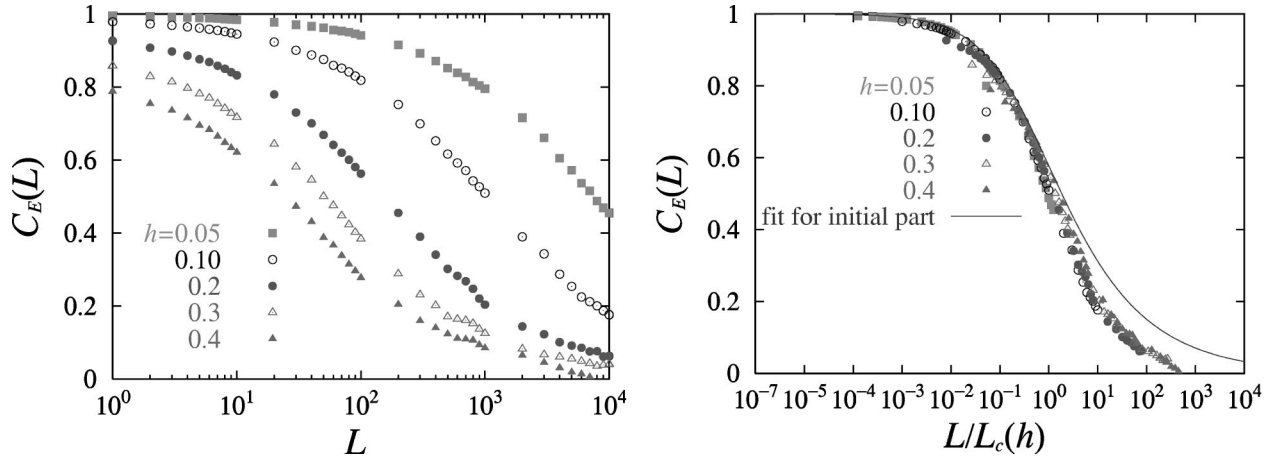


FIG. 3. $C_E(L)$ of the uniform tilt field case and its scaling plot with $L_c(h) = h^{-3}$. The fit is $C_F(L) = 1/(1 + A[L/L_c(h)]^{2(2/3-1/3)})$ with $A \sim 2.0$.

$$\Delta F_A(L) = F_A(L) - \overline{F_A(L)}, \quad \Delta F_B(L) = F_B(L) - \overline{F_B(L)}. \quad (111)$$

We also computed the overlap function $q(L, \delta U)$ defined in Eq. (39) using the method of [24]. However it requires much computational effort because one has to keep track of the trajectories of the two strings simultaneously and computation was limited to smaller system sizes $L \sim 500$. So we do not display the result in the following. We only note that the anticipated scaling (40) was checked within the limited system sizes.

A. Uniform tilt field

First, we examine the case of the perturbation by a uniform tilt field. For simplicity, the temperature is set to zero, $T=0$. The two replicas have exactly the same random potential. The difference is that replica B is subjected to a uniform tilt field h , which amounts to a force acting just on its end

$$E_A[V, h_A=0, u_A] = \sum_{z=1}^L V(u_A(z), z),$$

$$E_B[V, h_B=h, u_B] = \sum_{z=1}^L [V(u_B(z), z)] - hu_B(L). \quad (112)$$

We have used the $T=0$ transfer-matrix method and obtained the ground states with various perturbation strengths: $h = 0, 0.05, 0.1, 0.2, 0.3, 0.4$ for each realization of the random potential.

Let us begin with the mean-squared transverse displacement of the end point due to perturbation $B_2(L)$ defined in Eq. (109). $B_2(L)$ is expected to grow with increasing size L as $L^{1+2/3=5/3}$ in the weakly perturbed regime [see Eq. (33)] and as L^2 in the strongly perturbed regime [see Eqs. (37) and (36)]. Here we used the exponent associated with this perturbation $\alpha = \zeta = 2/3$ (see Sec. IV A). The crossover between the two is expected to take place at the overlap length $L_c \sim h^{-3}$ given in Eq. (18).

In Fig. 2, the data of $B_2(L)$ and its scaling plot is shown. For very weak perturbations $h=0.05$, the data grows almost entirely as $L^{1+2/3}$ except for a short length transient. On the contrary, the data corresponding to the strongest perturbation $h=0.4$ grows almost entirely as L^2 , again except for a short length transient. The data for the intermediate range of h displays a crossover between the two. Indeed, the scaling plot confirms the expected crossover scaling between the two regimes with no adjustable parameters.

Next let us examine the correlation of the ground-state energies of the perturbed and unperturbed systems through (110). In Fig. 3, the data of the correlation function and its scaling plot is shown. The data shows a decorrelation of the (free-) energy landscape of the two systems as expected. The scaling plot is obtained again without any adjustable parameters. The initial part of the master curve is well fitted by the expected form (46) using $\alpha = 2/3$, $C_L(F) = 1/(1 + A[L/L_c(h)]^{2(\alpha-1/3)})$ with $A \sim 2.0$. Note that the decay is faster for $L/L_c(h) \gg 1$.

B. Modified Sinai model

In Sec. VI we proposed a modified Sinai model as an effective model for the free ends of DPRM under uniform tilt field. Here we study numerically the properties of ground states of the modified Sinai model and the mean-squared displacement corresponding to Eq. (109) and the correlation function of the ground-state energies corresponding to Eq. (110). The effective Hamiltonian given in Eqs. (106) and (107) at a given length L reads [59,60]

$$H = H_A + H_B, \quad H_A = \frac{1}{2L} x_A^2 + \mathcal{V}(x_A),$$

$$H_B = \frac{1}{2L} x_B^2 + \mathcal{V}(x_B) - hx_B \quad (113)$$

where $\mathcal{V}(x)$ is the modified Sinai potential with correlations,

$$\overline{(\mathcal{V}(x) - \mathcal{V}(y))^2} = u + [u^*(L) - u] \theta(u - u^*(L))$$

with

$$u^*(L) = L^{2/3}. \quad (114)$$

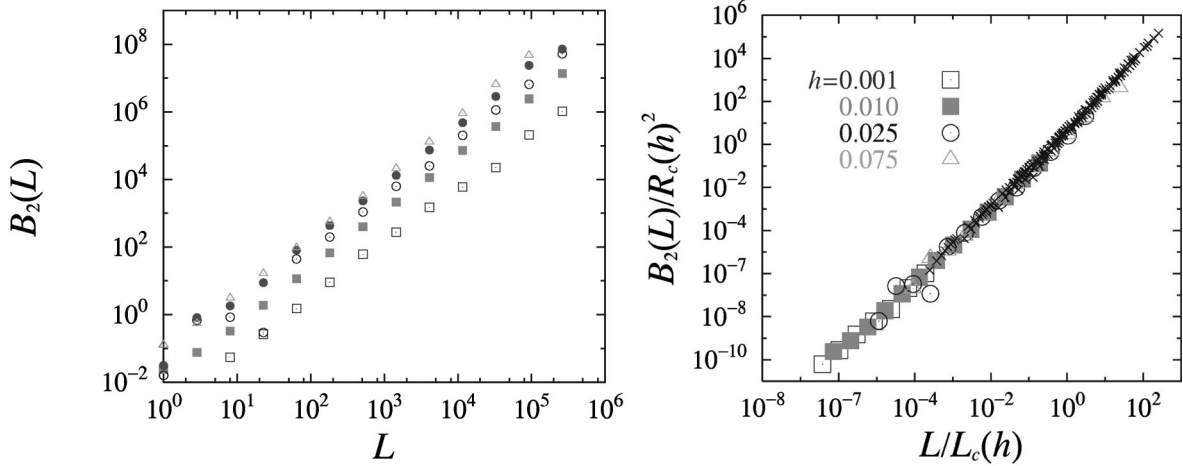


FIG. 4. $B_2(L)$ computed by the modified Sinai model and its scaling plot with $R_c(h) = (0.9h)^{-2}$. In the scaling plot, the master curve of DPRM under uniform tilt field plotted vs $L/L_c(h)$ as in Fig. 3 is also included for comparison (black points).

First we prepared the Sinai potential $V(x)$ on a one-dimensional lattice $u=1, 2, \dots, R$ of size R by generating random walks in one-dimensional space (regarding the one-dimensional space coordinate as the “time” coordinate for the random walk). We generated the *bounded* Sinai potential by a one-dimensional random walk confined in a box of size u^* . Each step of the random walk has variance 1. The same random potential is generated for two replicas A and B . For replica B , we add an extra tilting potential $-hu$. Then we numerically looked for the ground states of replicas A and B . We examined various system sizes up to $R=10^4$ and used 10^4 samples for the disorder averages.

The second moment of the distance between the minimum is computed for various L and h as

$$B_2(L) = \overline{[u_A^{\min}(L) - u_B^{\min}(L)]^2}. \quad (115)$$

In Fig. 4, the mean-squared displacement is shown together with the scaling plot. In the scaling plot, we included the master curve of the equivalent DPRM problem shown in Fig. 2. We used the anticipated scaling factors $L_c(h) = (0.9h)^{-3}$

and $R_c(h) = 1.2h^{-4}$. The numerical prefactors are chosen such that the master curve of the modified Sinai model lies on that of the DPRM problem.

The correlation function of the fluctuation of ground-state energies is computed for various L and h as

$$C_E(L) = \frac{\overline{\Delta E_A(L)\Delta E_B(L)}}{\sqrt{\overline{\Delta E_A^2(L)}}\sqrt{\overline{\Delta E_B^2(L)}}}, \quad (116)$$

where $\Delta E(L)$ is the deviation of a ground-state energy from the mean ground-state energy. In Fig. 5 we show the correlation function of the fluctuation of the ground-state energy as well as its scaling plot using the anticipated scaling variable $L/L_c(h)$. In the plot, we have included the master curve of the equivalent DPRM problem shown in Fig. 3.

It can be seen that the agreement between the modified Sinai model and the original DPRM under uniform tilt field is good. We checked that if the original unbounded Sinai potential is used, the agreement becomes very bad for large length scales. Especially, the correlation function $C_E(L)$

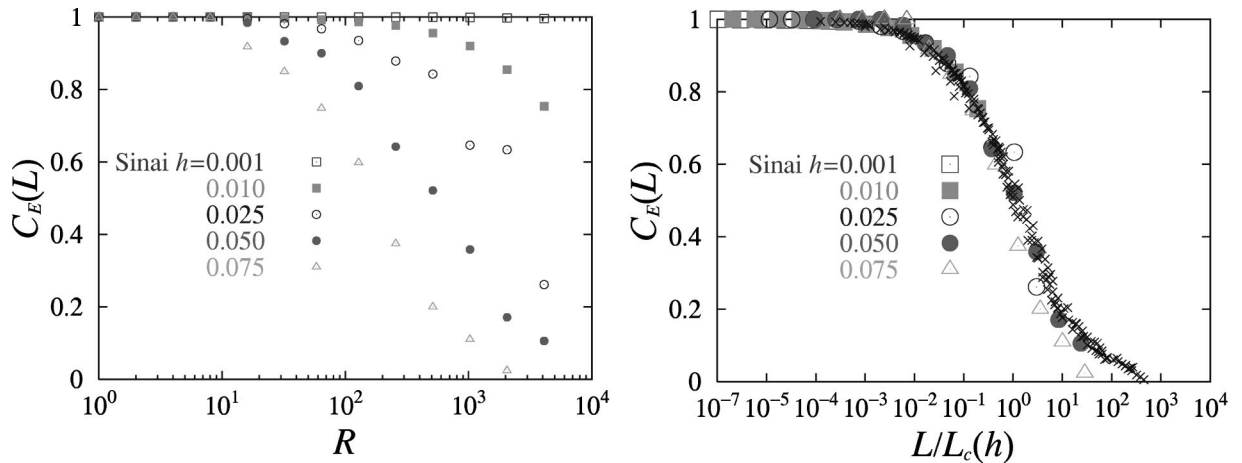


FIG. 5. $C_E(L)$ of Sinai model under uniform tilt field and its scaling plot with $R_c(h) = (0.9h)^{-2}$. In the scaling plot, the master curve of DPRM under uniform tilt field plotted vs $L/L_c(h)$ as in Fig. 3 is also included for comparison (black points).

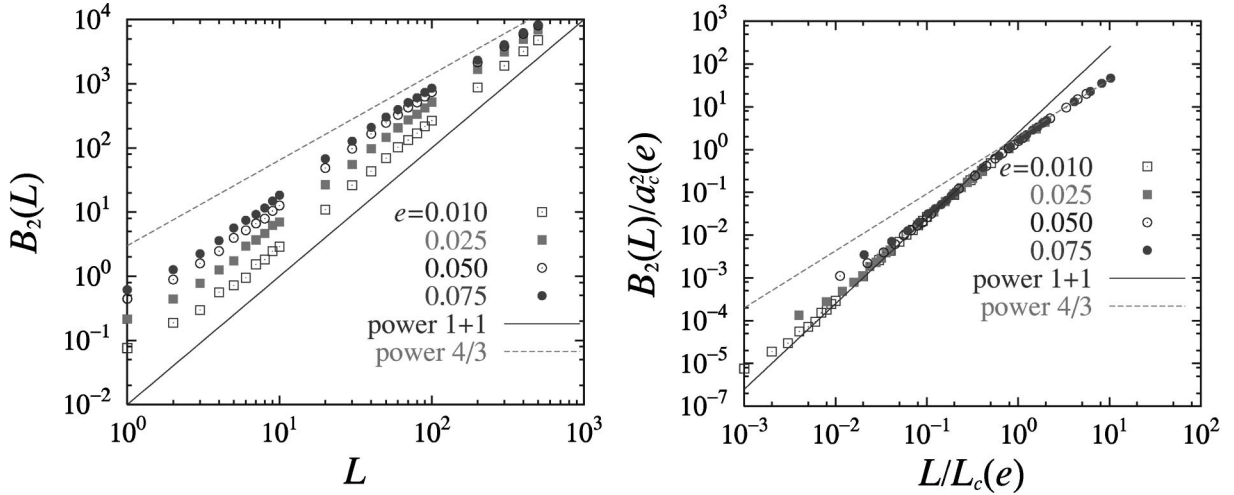


FIG. 6. $B_2(L)$ of the explicit repulsive coupling case and its scaling plot. Here the scaling parameters are $L_c(\epsilon) = \epsilon^{-3/2}$ and $u_c(\epsilon) = L_c(\epsilon)^{\zeta=2/3}$.

tends to saturate. These results support the picture that RSB is needed to account for the decorrelation of the energy landscape of DPRM under uniform tilt field.

C. Explicit repulsive coupling

Next we consider the case of explicit repulsive coupling. The two replicas are at zero temperature, have exactly the same random potential, and are coupled by an explicit repulsive coupling ϵ ,

$$E[V, V, \epsilon, u_A, u_B] = \sum_{z=1}^L [V(u_A(z), z) + V(u_B(z), z) + \epsilon \delta_{u_A(z), u_B(z)}]. \quad (117)$$

Here $\epsilon > 0$ is the strength of the perturbation. Mézard [24] proposed a transfer-matrix method to deal with such a coupled system at $T > 0$. Here we used a $T = 0$ version of the method and studied the ground states with different repulsive couplings $\epsilon = 0.05, 0.07, 0.1, 0.2, 0.3$.

In Fig. 6 the data of the mean-squared distance of the end points of the two replicas $B_2(L)$ is shown together with its scaling plot. From the discussion in Sec. IV D, it is expected to grow with increasing size L as $L^{1+1=2}$ in the weakly perturbed regime and $L^{4/3}$ in the strongly perturbed regime. Here we have used the exponent of the perturbation corresponding to the explicit repulsive coupling perturbation $\alpha = 1$ found in Sec. IV B [which is related to the order of the perturbation $p = 2$ in the replica analysis in Sec. V A]. The crossover between both regimes is expected to take place at the overlap length $L_c \sim \epsilon^{-2/3}$ given in Eq. (20). These features are well confirmed by the data and the scaling plot.

In Fig. 7, the correlation of the energies of the two replicas $E_A = \sum_{z=1}^L V(u_A(z), z)$ and $E_B = \sum_{z=1}^L V(u_B(z), z)$ is shown together with its scaling plot. The initial part of the master curve matches properly with the expected form (46) using $\alpha = 1$, $C_L(F) = 1/(1 + A[L/L_c(h)]^{2(1-1/3)})$ with $A \sim 0.35$. For $L/L_c(h) \gg 1$ the decay is much faster.

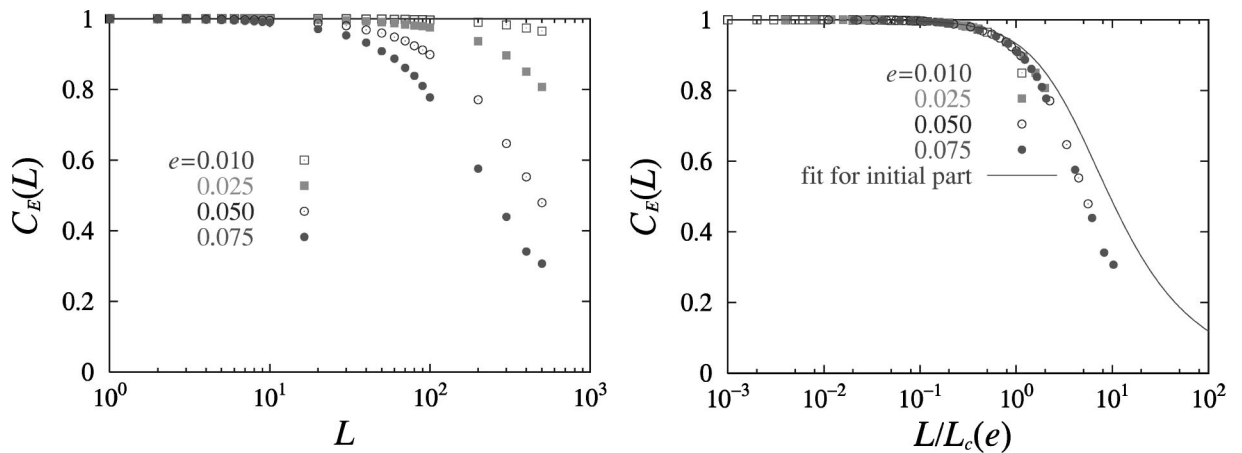


FIG. 7. $C_E(L)$ of the explicit repulsive coupling case and its scaling plot. Here the scaling parameter is $L_c(\epsilon) = \epsilon^{-3/2}$. The fit is $C_F(L) = 1/(1 + A[L/L_c(h)]^{2(1-1/3)})$ with $A \sim 2.0$.

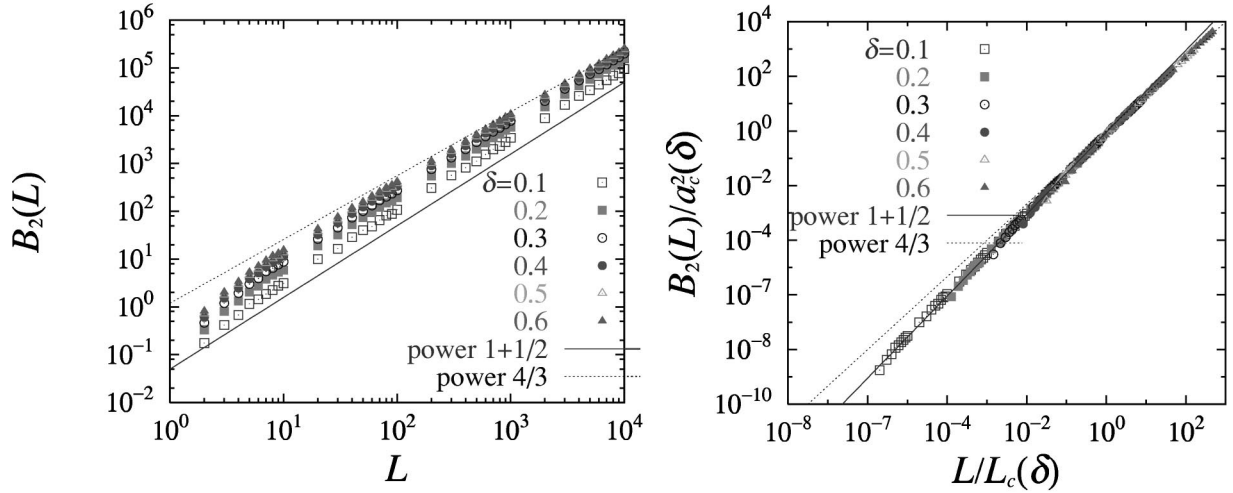


FIG. 8. $B_2(L)$ of the potential perturbation case and its scaling plot with $L_c(\delta) = \delta^{-6}$ and $u_c(\delta) = L_c(\delta)^{\xi=2/3}$.

D. Perturbation on temperature, random potential, and random tilt field

Finally we examine the class of perturbations which include temperature shift, potential change, and random tilt field. These perturbations are characterized by the exponent $\alpha = 1/2$ found in Sec. IV C (which is related to the order of the perturbation $p=2$ in the replica analysis in Sec. V A). Our primary interest here is to clarify whether these apparently different perturbations indeed lead to the same universal scaling properties as anticipated by the analytical arguments based on the replica-symmetry breaking *Ansatz*.

(1) *Potential change*. The Hamiltonian is given as

$$E_A[V, u_A] = \sum_{z=1}^L V(u_A(z), z),$$

$$E_A[V', u_B] = \sum_{z=1}^L V'(u_B(z), z). \quad (118)$$

The temperature is set to zero, $T=0$. First we generate a random potential $V(u, z)$ with random numbers drawn from

a uniform distribution between -1 and 1 . This is the potential for replica A . In order to construct the perturbed random potential for replica B , we draw another independent random number $U(u, z)$ from the same distribution and define

$$V'(u, z) = \frac{V(u, z) + \delta U(u, z)}{\sqrt{1 + \delta^2}}, \quad (119)$$

where δ is the strength of the perturbation. We have used the $T=0$ transfer-matrix method and examined the ground states for different strengths of the perturbation $\delta = 0.1, 0.2, 0.3, 0.4, 0.5, 0.6, 0.8, 1.0, 1.2$.

(2) *Random tilt field*. The Hamiltonian is given by

$$E_A[V, u_A, h_A=0] = \sum_{z=1}^L V(u_A(z), z) E_B[V, u_B, h_B]$$

$$= \sum_{z=1}^L [V(u_B(z), z)] - \delta \sum_{z=1}^{L-1} h_B(z)$$

$$\times (u_B(z+1) - u_B(z)). \quad (120)$$

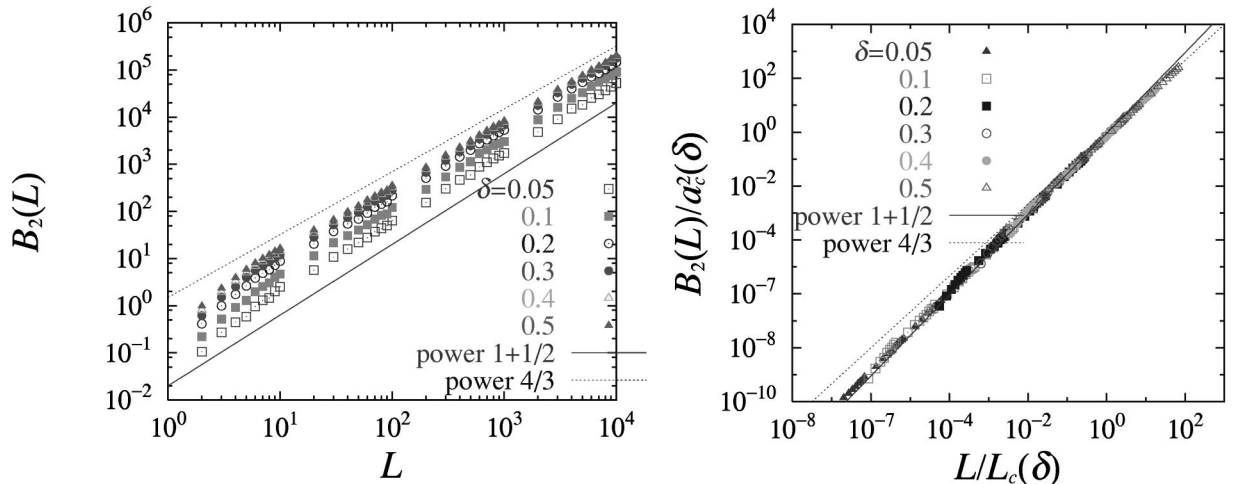


FIG. 9. $B_2(L)$ of the random tilt field perturbation case and its scaling plot with $L_c(\delta) = (0.87\delta)^{-6}$ and $u_c(\delta) = L_c(\delta)^{2/3}$.

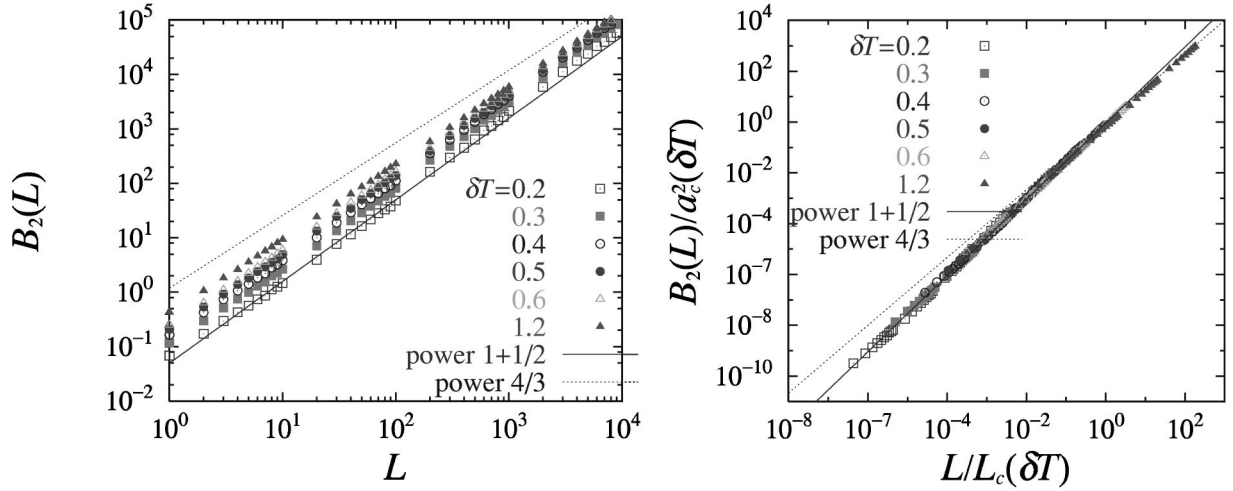


FIG. 10. $B_2(L)$ of the temperature-shift perturbation case and its scaling plot with $L_c(\delta T) = (0.43\delta T)^{-6}$ and $u_c(\delta T) = L_c^{2/3}(\delta T)$.

The temperature is set to zero, $T=0$. The two replicas have the same random potential $V(u, z)$. The difference is that replica B is subjected to a random tilt field $h_B(z)$, which for each z takes a different random value that is drawn from a uniform distribution between -1 and 1 . We have used the $T=0$ transfer-matrix method to examine the ground states with different random tilt intensities $\delta = 0.1, 0.2, 0.3, 0.4, 0.5$ for each realization of the random potential.

(3) *Temperature shift.* In the case of temperature perturbation, the Hamiltonian of A and B replicas are exactly the same,

$$E_B[V, u_A] = \sum_{z=1}^L V(u_A(z), z), \quad E_B[V, u_B] = \sum_{z=1}^L V(u_B(z), z). \quad (121)$$

We have used the finite temperature version of the transfer-matrix method. The temperature of replica A is set to $T_A = 0.1$. The temperature of replica B is varied as $T_B = T_A + \delta T$ with different temperature shifts $\delta T = 0.1, 0.2, 0.3, 0.4, 0.5, 0.6, 1.2$.

1. Transverse jumps

Let us first examine the mean-squared transverse displacement of the end point $B_2(L)$ due to this class of perturbations. By substituting $\alpha = 1/2$ in Eq. (33) we see that $B_2(L)$ is expected to grow with increasing size L as $L^{1+(1/2)=3/2}$ in the weakly perturbed regime. In the strongly perturbed regime, it should grow as $L^{4/3}$, as discussed in Sec. IVD 2, which is slightly slower than the growth in the weakly perturbed regime. The difference between exponents is of only $1/6$. The crossover between both regimes is expected to take place at the overlap length $L_c \sim L_0 \delta^{-6}$ as in Eqs. (23), (31), and (36) with δ being the strength of the perturbation.

In Figs. 8–10 the data for $B_2(L)$ corresponding to the three perturbations are shown together with their scaling plots. In the scaling plots we have chosen an adequate numerical prefactor c in $L_c(\delta) = (c\delta)^{-6}$ in order that the master curves corresponding to the three perturbations lie on the same curve. The resultant master curves become indistinguishable: the expected crossover behavior between weak

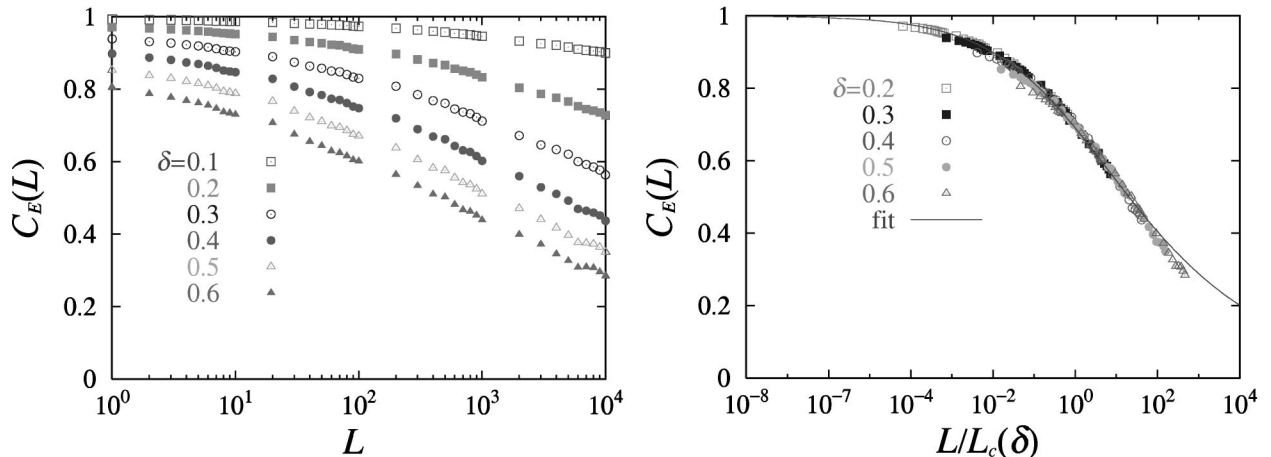


FIG. 11. $C_E(L)$ of the potential perturbation case and its scaling plot with $L_c(\delta) = (\delta)^{-6}$.

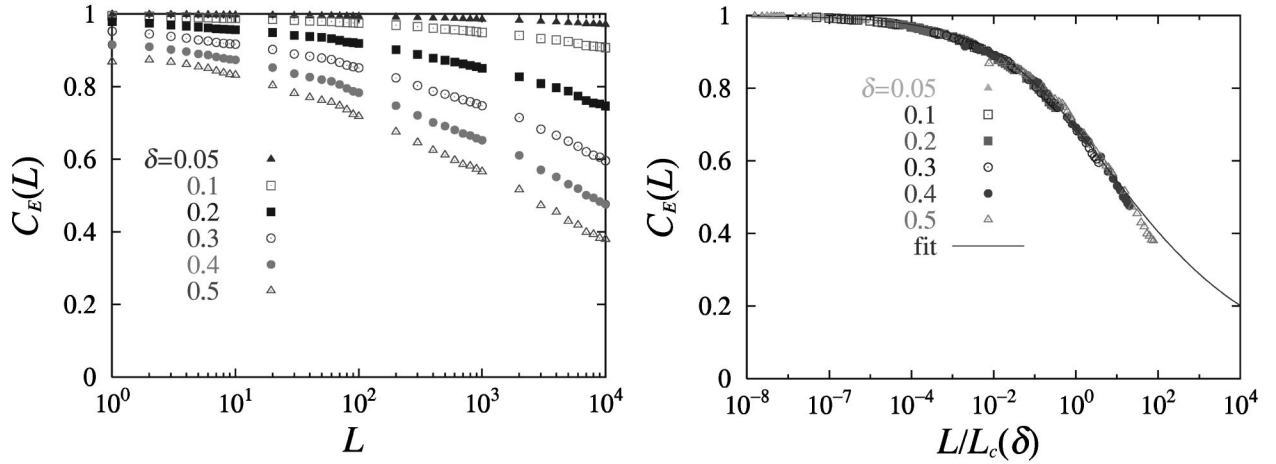


FIG. 12. $C_E(L)$ of the random tilt field perturbation case and its scaling plot with $L_c(\delta) = (0.87\delta)^{-6}$.

and strong perturbation regimes is indeed the *same* for the three kinds of apparently different looking perturbations.

2. Decorrelation of fluctuations of free energies and ground-state energies

In Figs. 11–13, the correlation of the the ground-state energies or free energies of the perturbed and unperturbed systems are shown together with their scaling plots. In the scaling plots we have used the same numerical prefactor c in $L_c(\delta) = (c\delta)^{-6}$ used in the scaling plot of $B_2(L)$. As one can see, the master curves for the three perturbations merge. The initial part of the master curve fits nicely into the expected form (46) using $\alpha = 1/2$, $C_L(F) = 1/(1 + A[L/L_c(h)]^{2(1-1/3)})$ with $A \sim 1.5$. One can see that the decay is faster for $L/L_c(h) \gg 1$. To sum up, the expected crossover behavior from the weakly perturbed regime and the strongly perturbed regime is indeed the same for the three kinds of apparently different perturbations.

VIII. CONCLUSION

In this work we have studied the sensitivity of the glassy phase of DPRM against various types of thermal and non-thermal perturbations. We have obtained very coherent re-

sults that strongly support the picture anticipated by the phenomenological scaling arguments. As we increase the length scale L at which observations are made, there is a crossover from the weakly perturbed regime dominated by rare events (i.e., jumps between neighboring free-energy valleys), $L \ll L_c(\delta)$, to the strongly perturbed regime where these events become typical, $L \gg L_c(\delta)$. This means that perturbations become strong at large length scales $L/L_c(\delta) \rightarrow \infty$ such that the configuration can easily jump from one valley to another, i.e., it becomes chaotic in the sense that the visited landscape is totally different from that before.

In replica space we proposed a definition of chaos, Eq. (5), in terms of the global partition function ($A+B$) rather than the correlation function itself. There is chaos if in the adequate limits the partition function factorizes, so that we have two noninteracting systems. The decorrelation of systems A and B when introducing a perturbation can be understood as a concrete example of explicit replica-symmetry breaking as proposed by Parisi and Virasoro [40]. Concerning the mapping to the Sinai model, it means that the free-energy landscape of the perturbed DPRM cannot be described anymore by a single Sinai potential. Instead, RSB requires the coexistence of statistically independent Sinai potentials.

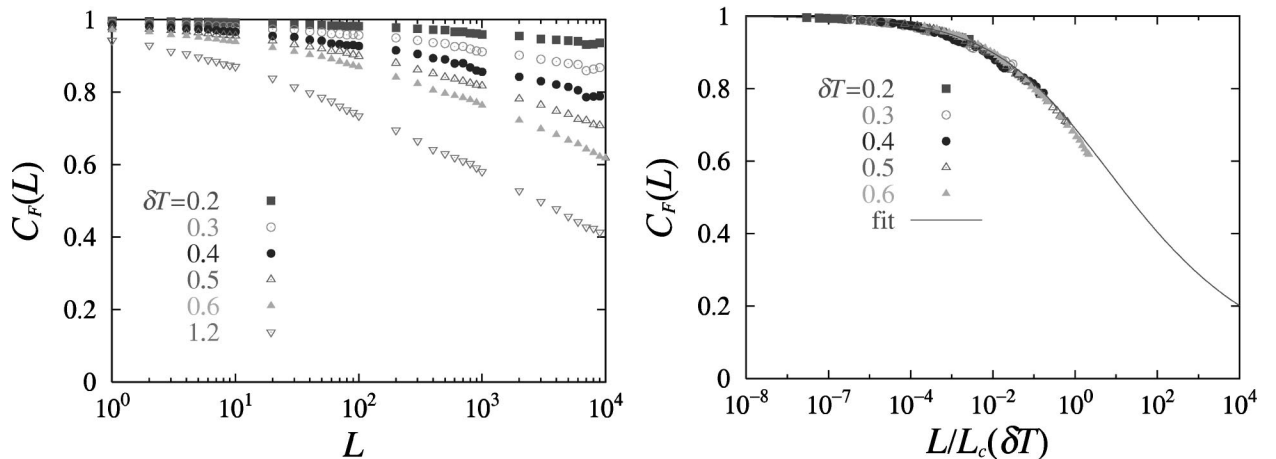


FIG. 13. $C_F(L)$ of the temperature-shift perturbation case and its scaling plot with $L_c(\delta T) = (0.43\delta T)^{-6}$.

The key point in our DPRM case is the fact that the RS bound state of the quantum problem is marginally stable with respect to RSB as noticed by Parisi [46]. Infinitesimally weak perturbations $\Delta \ll 1$ induce small replica-symmetry breaking terms and induce a symmetry breaking transition from a RS to a RSB state, which takes place in the $n/n^*(\Delta) \rightarrow 0$ limit for any small but nonzero strength of the perturbation. It turns out that we can read off the overlap length $L_c(\delta)$ from $n^*(\Delta)$. Within the replica space, the perturbations are naturally classified according to their order of perturbation p and the symmetries which are left conserved. For each class we have numerically verified that, indeed, there are universal scaling functions of correlation functions in terms of $L/L_c(\delta)$ describing the crossover from the weakly to strongly perturbed regimes. It is notable that the decay of the free-energy fluctuation $C_F(L)$ is very slow in all the cases we studied. It will not be surprising that one cannot have an impression of chaos by only making observations within some limited length scales.

In mean-field models, RSB is always associated with the existence of many pure states [45], which is not the case in DPRM in a strict sense. In the DPRM, the mapping to quantum mechanics is always possible for an arbitrarily large number of dimensions of the transverse space (usually denoted as N , being $N=1$ in our case) in which the ground state must contain the bosonic symmetry of the Schrödinger operator [61]. In this sense, RSB has to be *weak* in the DPRM problem [24,46], i.e., it is a latent feature that only manifests itself under certain circumstances. In the present $(1+1)$ -dimensional model the existence of a *hidden* RSB excited state with a vanishingly small gap with respect to the RS ground state in the $n \rightarrow 0$ limit is extremely important. Roughly speaking, the situation is not very far from having many pure states. In a really stable RS phase (such as ferromagnetic phases), this phenomena cannot happen. It is tempting to speculate that some lessons obtained in the present $(1+1)$ -dimensional DPRM case may turn out to be more general.

In the present paper, temperature chaos is confirmed. Thus, the present model serves as a suitable testing ground to examine the possible connection between temperature chaos and the restart of aging (rejuvenation) observed experimentally [6,7,62,63]. Experimentally, almost a complete restart of *aging* or relaxation takes place only due to slight temperature changes. Whether this restart of aging can be associated with temperature chaos remains an interesting open question. Interestingly enough, recent experiments [62,63] suggest the

rejuvenation (chaos) effect in random ferromagnetic systems. A candidate to account for the mechanism of the phenomena may be the temperature chaos of pinned domain walls of ferromagnets, which is directly related to the present study.

Another surprise revealed by the temperature-cycling experiments is that initial aging is resumed when the temperature is cycled back to the initial temperature, giving rise to the so-called memory effect. It appears contradictory to the temperature-chaos effect at first sight. Recently a coarsening model under cycling of target equilibrium states was studied [64]. There, a hidden *dynamical memory by ghost domains* was found and a scenario was proposed to explain the intriguing coexistence of the rejuvenation and memory effect. In the present context of pinned elastic manifold, rejuvenation and memory can be easily explained by considering Fourier components of the temporal configuration. When the temperature is shifted, Fourier components at wavelengths larger than the overlap length will be subjected to rejuvenation. At time t after the temperature shift, Fourier components at wavelengths shorter than $L(t)$ will be adopted to the new temperature. Here $L(t)$ is a dynamical length scale over which the system can be equilibrated within a given time t . However, Fourier components of an even larger wavelength [$>L(t)$] remain the same as before the temperature shift. Thus, *dynamical memory* exists at the coarse-grained level of $L(t)$.

Recalling that relaxational dynamics is extremely slow in glassy systems because of the dominance of the activated processes, one has to seriously consider how a large time scale is needed to go beyond the overlap length. If it is too large, even experimental time scales [typically $(10^{14} - 10^{17})\tau_0$, where $\tau_0 \sim 10^{-13}$ sec] may not be sufficient and one must look for other mechanisms [65–67] to explain the rejuvenation phenomena observed experimentally. Previous numerical studies of the relaxational dynamics of the present DPRM model [68] imply that the needed time lies within the time window of experiments and numerical simulations for some realistic parameters. More work in this direction would certainly be interesting.

ACKNOWLEDGMENTS

We thank the Service de Physique de l'État Condensé, CEA Saclay, where this work was begun, for their financial support and kind hospitality. M.S. acknowledges the MEC of the Spanish government for Grant No. AP98-36523875. We especially thank M. Mézard, J. P. Bouchaud, and F. Ritort for kind suggestions and many useful discussions.

-
- [1] A. J. Bray and M. A. Moore, Phys. Rev. Lett. **58**, 57 (1987).
 [2] D. S. Fisher and D. A. Huse, Phys. Rev. B **38**, 386 (1988); **38**, 373 (1988).
 [3] D. S. Fisher and D. A. Huse, Phys. Rev. B **43**, 10728 (1991).
 [4] J. Banavar and A. J. Bray, Phys. Rev. B **35**, 8888 (1987).
 [5] M. Ney-Nifle and H. J. Hilhorst, Phys. Rev. Lett. **68**, 2992 (1992); Physica A **193**, 48 (1993).
 [6] K. Jonason, E. Vincent, J. Hamman, J. P. Bouchaud, and P.

Nordblad, Phys. Rev. Lett. **81**, 3243 (1998).

- [7] E. Vincent, J. Hammann, and M. Ocio, *Recent Progress in Random Magnets* (World Scientific, Singapore, 1992); P. Nordblad and P. Svedlindh, in *Spin Glasses and Random Fields*, edited by A. P. Young Series on Directions in Condensed Matter Physics Vol. 12 (World Scientific, Singapore, 1998).
 [8] P. E. Jönsson, H. Yoshino, and P. Nordblad, e-print

- cond-mat/0203444.
- [9] F. Ritort, Phys. Rev. B **50**, 6844 (1994).
- [10] V. Azcoiti, E. Follana, and F. Ritort, J. Phys. A **28**, 3863 (1995).
- [11] H. Rieger, L. Santen, U. Blasum, M. Diehl, and M. Jünger, J. Phys. A **29**, 3939 (1996).
- [12] M. Ney-Nifle, Phys. Rev. B **57**, 492 (1997).
- [13] Sompolinski (unpublished) cited in p. 886 of K. Binder and A. P. Young, Rev. Mod. Phys. **58**, 801 (1986).
- [14] I. Kondor, J. Phys. A **22**, L163 (1989).
- [15] I. Kondor and A. Végö, J. Phys. A **26**, L641 (1993).
- [16] S. Franz and M. Ney-Nifle, J. Phys. A **28**, 2499 (1995).
- [17] T. Rizzo, J. Phys. A **34**, 5531 (2001).
- [18] D. A. Huse and L-F. Ko, Phys. Rev. B **56**, 14597 (1997).
- [19] A. Billoire and E. Marinari, J. Phys. A **33**, L265 (2000).
- [20] R. Mulet, A. Pagnani, and G. Parisi, Phys. Rev. B **63**, 184438 (2001).
- [21] A. Billoire and E. Marinari, e-print cond-mat/0202473.
- [22] M. Sales and H. Yoshino, e-print cond-mat/0112384.
- [23] For a review of directed polymer in random media, see T. Halpin-Healy and Y. C. Zhang, Phys. Rep. **254**, 215 (1995).
- [24] M. Mézard, J. Phys. I **51**, 1831 (1990).
- [25] Y. C. Zhang, Phys. Rev. Lett. **59**, 2125 (1987).
- [26] M. V. Feigel'man and V. M. Vinokur, Phys. Rev. Lett. **61**, 1139 (1988).
- [27] Y. Shapir, Phys. Rev. Lett. **66**, 1473 (1991).
- [28] T. Halpin-Healy and D. Herbert, Phys. Rev. E **48**, R1617 (1993).
- [29] M. Mézard and G. Parisi, J. Phys. I **1**, 809 (1991).
- [30] L. Balents and D. S. Fisher, Phys. Rev. B **48**, 5949 (1993).
- [31] L. Balents, J. P. Bouchaud, and M. Mézard, J. Phys. I **6**, 1007 (1996).
- [32] T. Giamarichi and P. Le. Doussal, Phys. Rev. Lett. **72**, 1530 (1994); Phys. Rev. B **52**, 1242 (1995).
- [33] P. Chauve, T. Giamarichi, and P. Le Doussal, Phys. Rev. B **62**, 6241 (2000).
- [34] D. A. Huse and C. L. Henley, Phys. Rev. Lett. **54**, 2708 (1985).
- [35] S. Lemerle, J. Ferré, C. Chappert, V. Mathet, T. Giamarichi, and P. Le Doussal, Phys. Rev. Lett. **80**, 849 (1998).
- [36] G. Blatter, M. V. Feigel'man, V. B. Genkenbein, A. I. Larkin, and V. M. Vinokur, Rev. Mod. Phys. **66**, 1125 (1994).
- [37] C. A. Bolle *et al.*, Nature (London) **399**, 43 (1999).
- [38] H. Fukuyama and P. A. Lee, Phys. Rev. B **17**, 535 (1978).
- [39] G. Grüner, Rev. Mod. Phys. **66**, 1129 (1988).
- [40] G. Parisi and M. A. Virasoro, J. Phys. (France) **50**, 3317 (1989).
- [41] M. Kardar, Nucl. Phys. B **290**, 582 (1987).
- [42] M. Kardar, in *Proceedings of Fluctuating Geometries in Statistical Mechanics and Field Theory*, edited by F. Daivid, P. Ginzparg, and J. Zinn-Justin (Elsevier, Amsterdam 1996).
- [43] D. A. Gorokhov and G. Blatter, Phys. Rev. Lett. **82**, 2705 (1999).
- [44] G. Parisi, J. Phys. A **13**, L115 (1980); **13**, 1101 (1980); **13**, 1887 (1980).
- [45] M. Mézard, G. Parisi, and M. A. Virasoro, *Spin-Glass Theory and Beyond* (World Scientific, Singapore, 1988).
- [46] G. Parisi, J. Phys. I **51**, 1595 (1990).
- [47] A. I. Larkin, Sov. Phys. JETP **31**, 784 (1970).
- [48] In the spin-glass problems the chaos exponent is denoted as ζ . Here we do not use the convention because it is usually used for the roughness exponent ζ .
- [49] We observed the following numerically within the lattice model we used in Sec. VII D. We computed root-mean-square average of the sample-to-sample fluctuations of energy, entropy, and free energy. Fluctuation of energy with respect to the mean value depends on temperature T as $\sqrt{[\Delta E(L)]^2} = U_0(L/L_0)^\theta + ck_B T(L/L_0)^{1/2}$, where c is a numerical constant. Note that the $L^{1/2}$ behavior shows up only at sufficiently large length scales (as found in [3]). The temperature dependence is consistent with the observation that fluctuation of energy at $T=0$ (ground state) scales as $\lim_{T \rightarrow 0} \sqrt{[\Delta E(L)]^2} = U_0(L/L_0)^\theta$, which is often assumed in the scaling arguments. On the other hand the entropic fluctuation scales as $\sqrt{[S(L)]^2} = c(L/L_0)^{1/2}$, which is consistent with the observation that the fluctuation of free energy $\Delta F = \Delta E - k_B T \Delta S$ scales as $\sqrt{[\Delta F(L)]^2} = U_0(L/L_0)^\theta$.
- [50] G. Forgacs, R. Lipowsky, and Th. M. Nieuwenhuizen, in *Phase Transitions and Critical Phenomena*, edited by C. Domb and J. Lebowitz (Academic Press, Kondon, 1991), Vol 14.
- [51] T. Hwa and D. S. Fisher, Phys. Rev. B **49**, 3136 (1994).
- [52] U. Schulz, J. Villain, E. Brézin, and H. Orland, J. Stat. Phys. **51**, 1 (1988).
- [53] J. P. Bouchaud and H. Orland, J. Stat. Phys. **61**, 877 (1990).
- [54] D. A. Huse, C. L. Henley, and D. S. Fisher, Phys. Rev. Lett. **55**, 2924 (1985).
- [55] To treat the replica number n as a scaling variable has been proposed by several authors [23,42].
- [56] The choice of renormalized D in Eq. (82) allowed to simplify the calculation. One can work also with the original D and will find the same *positive* $\delta D(n,L)/L$ of order $O(n^2)$ up to some irrelevant differences.
- [57] Ya. G. Sinai, Theor. Probab. Appl. **27**, 247 (1982).
- [58] M. Kardar, Phys. Rev. Lett. **55**, 2923 (1985).
- [59] Note that here we do not use rescaled variables such as in Eq. (98).
- [60] The same results are obtained if we consider that the two strings are tilted with $-h$ and $+h$, respectively.
- [61] M. Mézard and G. Parisi, J. Phys. A **25**, 4521 (1992).
- [62] K. Jonasson, J. Mattson, and P. Nordblad, Phys. Rev. Lett. **77**, 2562 (1996); K. Jonason and P. Nordblad, Eur. Phys. J. B **10**, 23 (1999).
- [63] E. Vincent, F. Alet, J. Hammann, M. Ocio, and J. P. Bouchaud, Europhys. Lett. **50**, 674 (2000).
- [64] H. Yoshino, A. Lemaitre, and J. P. Bouchaud, Eur. Phys. J. B **20**, 367 (2000).
- [65] J-P. Bouchaud, in *Soft and Fragile Matter*, edited by M. E. Cates and M. R. Evans (Institute of Physics, Bristol, 2000); e-print cond-mat/9910387.
- [66] J. P. Bouchaud, V. Dupuis, J. Hammann, and E. Vincent, Phys. Rev. B **65**, 024439 (2001).
- [67] L. Bertheir and J.-P. Bouchaud, e-print cond-mat/0202069.
- [68] H. Yoshino, Phys. Rev. Lett. **81**, 1493 (1998); and (unpublished).